DENDROBIOLOGY

2022, vol. 87, 27–46

https://doi.org/10.12657/denbio.087.003

*Houyin Deng, Dehuo Hu, Ruping Wei, Shu Yan, Runhui Wang, Huiquan Zheng**

Global transcriptome analysis reveals genes associated with seedling advance growth traits in a selfed family of Chinese fir (*Cunninghamia lanceolata*)

Received: 15 August 2021; Accepted: 2 February 2022

Abstract: Chinese fir (*Cunninghamia lanceolata* (Lamb.) Hook.) is a major timber conifer species in southern China. In this study, we aimed to capture the rarely advanced phenomenon for selfing in this species and illustrated the underlying molecular mechanism, especially the hub gene-regulated networks and pathways, by global transcriptome analysis assays (RNA-Seq). Self-pollination trials revealed a wide variation of selfing effects among parents. Parent cx569 produced a selfed family with the best growth performance at the seedling stage. The growth-based extremely advanced (AD) (n=3) and depressed (DE) variants (n=3; different types) were then subjected to comparative RNA-Seq. The transcriptome data revealed more than 5000 differentially expressed genes (DEGs) for each comparison group (AD versus DE). Weighted gene co-expression network analysis (WGCNA) further identified more than 80 important DEGs that were significantly associated with growth traits in each comparison group. A subsequent enrichment analysis showed that the identified DEGs belonged to six main types, including xylem metabolism-related, sugar and energy metabolism-related, plant hormone signal transduction-related, stress response-related, cytochrome-related, and transcription factor genes. Ten hub genes represented by the *ERF071*, *MYB-relate 305*, *WRKY6*, *WRKY31*, *PER3*, *LAC4*, *CESA8*, *CESA9*, *GID1*, and *PR1* genes were co-identified between AD and DE variants. These genes exhibited rather different expression patterns between AD and DE variants, especially of the transcription factor *ERF071* gene that presented a low transcript level in the AD seedlings with only 4.45% activity compared to DE's. While, the plant hormone signal transduction *GID1* gene was significantly upregulated in AD by about 20-fold when compared to DE's, and fold change of the lignin biosynthesis-related *PER3*, *CESA9* and *LAC4* gene expression parallel reached to 10–15 times in an upregulation pattern in AD seedlings. The set of hub gene-linked interaction networks and pathways revealed in this study may be responsible for the rarely advanced phenomenon for selfing at the seedling stage in Chinese fir.

Keywords: Chinese fir, selfing, RNA-Seq, growth trait, hub gene

Addresses: H. Deng, D. Hu, R. Wei, S. Yan, R. Wang, H. Zheng, Guangdong Provincial Key Laboratory of Silviculture, Protection and Utilization; Guangdong Academy of Forestry, Guangzhou 510520, People's Republic of China, e-mail: zhenghq@sinogaf.cn
H. Deng, College of Biological Sciences and Biotechnology, Beijing Forestry University, Beijing 100083, People's Republic of China
*Corresponding author

Introduction

Selfing, the reproductive mode that involves male and female gametes from a single individual, is an extreme form of inbreeding (Cornetti et al., 2021). Currently, about 10–15% of flowering plants are predominantly reproduced by selfing and approximately 49% of plants maintain a mixed pollination mechanism of selfing and outcrossing (Vogler & Kalisz, 2001; Wright et al., 2013). Outcrossing can produce heterosis, whereas selfing can provide reproductive assurance (Wright et al., 2013; Shimizu & Tsuchimatsu, 2015). By selfing, plants can ensure the success of a single individual's fecundity when mates or pollinators are not available, and increase their ability to adapt to changes in climate, geography, and reproductive systems (Razanajatovo et al., 2016; Hartfield et al., 2017; Lesaffre & Billiard, 2020). Selfing can also increase the genetic variance between lines, thus increasing responses to phenotypic selection (McClosky et al., 2013). Furthermore, it is also possible to advance homozygosity while selecting for the most suitable and fertile phenotypes through selfing (Peterson et al., 2016). However, inbreeding depression is prevalent in plant kingdom (Del Castillo & Trujillo, 2008). Selfing often leads to inbreeding depression characterized by reduced survival and sterility, stunted growth and development, poor stress resistance, and even death (Charlesworth & Willis, 2009; Rymer et al., 2015). Inbreeding may have a strong influence on germination, seedling survival, and growth at the nursery stage (Liesebach et al., 2021). However, it is worth noting that individuals may vary in their genetic load due to different selfing histories, which can result in differences in inbreeding depression among families (Collin et al., 2009). As a result, selfing does not inevitably lead to inbreeding depression in some materials, and may even produce superior individuals (Cuénin et al., 2019). Some conifers, such as *Pinus radiata* and *Pinus taeda*, present selfing lines expressing excellent growth vigor in growth traits that has increased with the inbreeding level (Wu et al., 1998; Ford et al., 2015). To date, knowledge on the advanced phenomenon in plant selfing has been relatively limited. Capturing the advanced phenomenon for selfing and illustrating the underlying molecular mechanisms will further increase the understanding of selfing behaviors in the plant kingdom.

Early studies largely depended on expressed sequence tag sequencing methods (e.g., Sanger sequencing) for functional genomics research. These methods are costly, time-consuming, and sensitive to cloning biases (Huang et al., 2012). With the development of high-throughput features with accuracy and low cost, next-generation sequencing (NGS) is now being widely used for functional genomics research (Sharma & Shrivastava, 2016). The 'omic' technologies have provided an avenue for many biological research programs (Paige, 2010; Kristensen et al., 2010; Duangjit et al., 2013; García de la Torre et al., 2021; Yu et al., 2021). The NGS-based transcriptomics approach permits the identification of genes associated with inbreeding and may help unravel affected pathways (Menzel et al., 2015). To date, transcriptional analysis associated with inbreeding has been reported in many plant species, such as *Arabidopsis arenosa*, *Brassica rapa* L. ssp. Pekinensis, and *Camellia sinensis* (Zhang et al., 2016; Liu et al., 2018; Barragan et al., 2021). Furthermore, transcriptome analysis of grapevine self-bred progeny and crossed progeny has revealed that selfing involves the interaction of multiple genes and pathways in plant growth and development (Arro et al., 2017). Strikingly, several ecologically and economically important conifer tree species, including loblolly pine (*P. taeda* L.), Douglas fir (*Pseudotsuga menziesii*), and Norway spruce (*Picea abies* (L.) Karst.), have also been subjected to transcriptome assay to identify genes relevant to their growth characteristics (OuYang et al., 2015; Cronn et al., 2017; Mao et al., 2019).

The development of RNA sequencing (RNA-Seq) methodologies has enabled profiling of the transcriptome in different patterns of expression levels (Wang et al., 2009). In addition, the RNA-Seq approach can be used to efficiently identify all transcribed loci in a sample without requiring a priori knowledge of gene models (Wang et al., 2021). For analyzing expression data, powerful tools, such as weighted gene co-expression network analysis (WGCNA), are available for identifying central genes (hub genes) with important functions (Langfelder & Horvath, 2008). WGCNA has been widely used in plants to identify hub genes associated with growth and development, and is regarded as a powerful tool (Zou et al., 2019; Feng et al., 2021; Yue et al., 2021).

Chinese fir (*Cunninghamia lanceolata* (Lamb.) Hook.) is one of the major timber conifer species in southern China (Shi et al., 2010; Zheng et al., 2019). It is a monoecious species that usually exhibits a relatively high selfing rate, leading to inbreeding depression that tends to emerge at the seedling stage, but there is considerable variation in selfing responses among parents (Wang and Chen, 1988; Duan et al., 2017). Advanced phenomenon in selfing has been discovered in Chinese fir in some cases (e.g., volume growth) (Yu et al., 2008; Xu et al., 2015; He et al., 2016). We speculate that in some cases, the rarely advanced phenomenon for selfing may be observed in some families of Chinese fir. We propose that in this sense, the advanced (AD; higher vigor) and depressed (DE; lower vigor) variants from seedlings of selfed family in Chinese fir may be captured at an early stage of development. More experiments are required to test this hypothesis. Given a

strong selection against the selfing family in the early growth stage, herein, we conducted a self-pollination assay in Chinese fir and captured a potential advance family expressing elite growth traits at the seedling stage. The AD and depressed DE variants are obtained from selfed progenies of the potential advance family. Global transcriptome assays (RNA-Seq) and the WGCNA approach were then used on AD and DE variants from selfing seedlings with the aim to illustrate the underlying molecular mechanism, especially the hub gene-regulated networks and pathways responsible for the rarely advanced phenomenon (seedling growth) for selfing in Chinese fir.

Materials and methods

Plant materials

Six core parents (clone cx561, cx569, cx571, cx573, cx578, and cx580) were subjected to self-pollinated assay in a 2.5th generation seed orchard of Chinese fir that harbored 20 parents in the Xiaokeng State Forest Farm (Guangdong province, China; 24°70'N, 113°81'E, at an altitude of 328–339 m). The unpollinated female strobili of parent trees were bagged before the pollination fitness period to prevent contamination by exogenous pollen. In the self-pollination experiment, pollen from the same tree was injected into the bag with a syringe while the bagged branch was gently shaken to ensure that the pollen was deposited on receptive female strobili. The self-pollination assays were conducted with sufficient pure pollen and repeated twice, ensuring full pollination. The seeds (32–137.8 g) were then manually collected from the self-pollinated cones of each parent in November, 2016. Simultaneously, the open-pollinated seeds (about 80.0 g) were collected from the same tree for each parent. The cone-set and the cone-seed rate were estimated for each parent, and the thousand kernel weight, seed soundness, germination rate, and embryo abortion rate were also evaluated with a randomly selected seed lot (30 g per self- or open-pollinated family) that harbored around 4500 fresh seeds.

The germinated seeds were then transferred to peat soil mixed with 20% expanded-perlite, and maintained in a growth chamber at 25°C under a 16/8 h light/dark photoperiod with a humidity of 75%. The vigor of seedlings was estimated based on the traits of height (H), length of the longest root (LLR), number of roots (secondary roots) (RN), fresh weight of seedlings (FWS), fresh weight of the above-ground part (leaves and stems) (FWSL), and fresh weight of the roots (FWR). Only the best conserved self-pollinated family was measured for the traits. The cx569 self-pollinated family harbored advanced (AD) and depressed (DE) variants at seedling stage.

Transcriptional analysis (RNA-Seq)

Total RNA was extracted from the above-ground tissues (leaves and stems) of AD and DE variants with an SV Total RNA Isolation System (Promega, Madison, WI, USA). To ensure the use of quality samples for transcriptome sequencing, the purity, concentration, and integrity of the RNA samples were detected by Nanodrop, Qubit 2.0, and Agilent 2100 instruments, respectively. The concentration of RNA samples was all over 46.0 ng/ul. The RNA integrity numbers (RINs) of isolated RNA samples were measured, and samples with an RIN above 6.3 were used for RNA library construction. Each mRNA was isolated from total RNA using Dynabeads oligo (dT) (Invitrogen). Then, the enriched mRNA was fragmented into short fragments using fragmentation buffer and reverse transcribed into first-strand cDNA with random hexamers. Second-strand cDNA was synthesized by DNA polymerase I, RNase H, dNTP, and buffer. The cDNA strand was purified using AMPure XP beads, end repaired, poly(A) tail added, and ligated to Illumina sequencing adapters, and then the fragment size was selected by AMPure XP beads. The cDNA libraries were subsequently constructed by polymerase chain reaction and quantified by quantitative real-time polymerase chain reaction to acquire the effective libraries. Finally, the effective libraries were sequenced to generate paired-end transcriptome reads (raw RNA-Seq reads) using the Illumina system HiSeq XTen platform provided by Biomarker Biotechnologies Corporation (Beijing, China, www.biocloud.net). The read length was 150-bp double-ended reads.

Bioinformatic analysis

To obtain high-quality reads, the raw RNA-Seq reads were filtered with fastp software to remove low-quality reads, short reads, and adapters (Chen et al., 2018). The clean reads were then de novo assembled in Trinity v2.5.1 (Haas et al., 2013). Sequence alignment was performed using bowtie (Langmead & Salzberg, 2012). The mapped reads were used for subsequent analysis.

Gene expression levels (fragments per kilobase of transcript per million mapped read, FPKM) were estimated by RSEM for each sample (Li & Colin, 2011). Spearman's correlation analysis and principal component analysis (PCA) using the $\log_{10}$ (FPKM+1) of all unigenes were used to reveal the transcription pattern between each sample. The false discovery rate (FDR) was controlled using the Benjamini and Hochberg approach to adjust the *P*-values (Benjamini & Hochberg, 1995). Prior to differential gene expression analysis, for each sequenced library, the read counts were adjusted by EBSeq R package

through one scaling normalized factor. Based on adjusted read counts, differential expression analysis of two samples between AD and DE variants were performed to obtained differentially expressed genes (DEGs) using the EBSeq R package with the cut-off *P*-adjust (FDR) < 0.01 and $|\log_2$ FC (fold change, FC) | > 1. BLAST was used to align genes to a series of protein databases, including the Non-redundant (Nr) NCBI (Deng et al., 2006), Swiss-Prot (Apweiler et al., 2004), Gene Ontology (GO) (Ashburner et al., 2000), Clusters of Orthologous Groups (COG) (Tatusov et al., 2000), EuKaryotic Orthologous Groups (KOG) (Koonin et al., 2004), Kyoto Encyclopedia of Genes and Genomes (KEGG) (Kanehisa et al., 2004), and Pfam (Finn et al., 2014) databases.

A WGCNA was performed to construct the genetic co-expression networks regarding the relationships between the unigenes and morphological traits (Langfelder & Horvath, 2008). GO enrichment and KEGG enrichment analyses were conducted using the topGO R package and Clusterprofiler R package, respectively (Alexa & Rahnenfuhrer, 2010; Yu et al., 2012). TBtools was then used to generate heatmaps based on DEG data (Chen et al., 2020). Correlation analysis based on DEG data was conducted to estimate the correlation coefficients between each DEG using the R package corrplot (Wei & Simko, 2017). Only the DEGs paired with an absolute value of correlation coefficient > 0.8 were considered as having a high correlation, and these partial DEG pairs were used to construct a gene regulatory network using Cytoscape software version 3.7.1 (Shannon et al., 2003).

Results

Selfing assays revealed an elite family with advanced growth traits at the seedling stage

The results of cone development after cone ripening were characterized by normal cone and cone abortion based on self-pollination assays (Fig. 1). The self-pollinated cone-set rate was higher than 64.6% in the tested Chinese fir parents (n=6), with the highest rate found in parent cx569 (86.7%). The self-pollinated

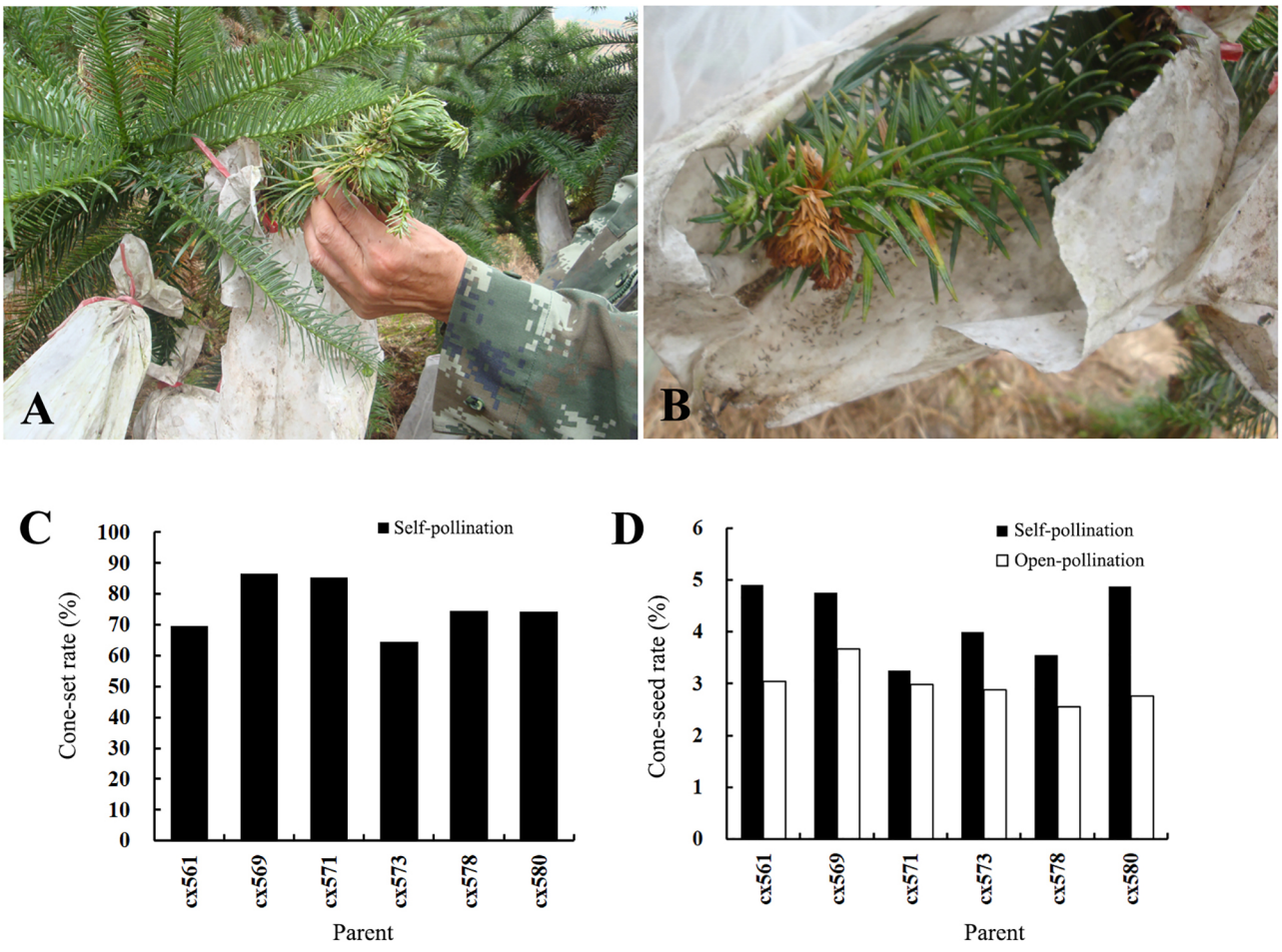

Fig. 1. The result of cone growth and development in tested parents. (A) Selfing cone-set. (B) Self-infertility. (C) Cone-set rate in six Chinese fir parents (clone 561, cx569, cx571, cx573, cx578, and cx580). (D) Cone-seed rate in the tested samples between self- and open-pollination assays

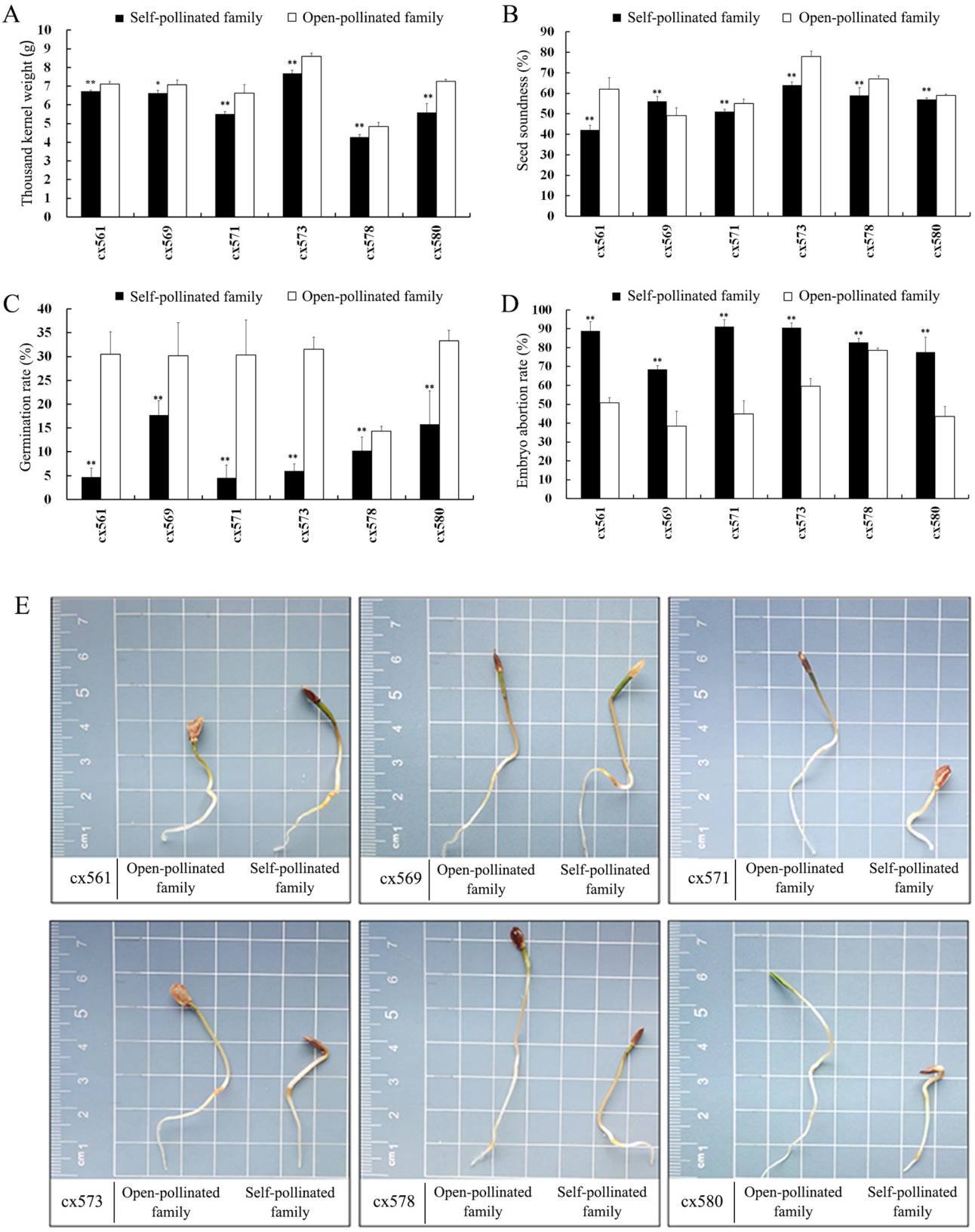

Fig. 2. Comparison of the quality of the self-pollinated family with that of the open-pollinated family in six Chinese fir parents (clone cx561, cx569, cx571, cx573, cx578, and cx580). (A)–(D) Thousand kernel weight, seed soundness, germination rate, and embryo abortion rate, respectively, of the self-pollinated and open-pollinated family. The data are shown as means ± standard deviation (SD). Student's t-test was used to test for statistical significance (*$P < 0.05$; **$P < 0.01$) between the self-pollinated family and the open-pollinated family in the same parent. (E) The optimal seedling growth of the self- and open-pollinated families in samples (14 days after sowing)

cone-seed rate (3.3–4.9%; mean=4.2%) was higher than that of the corresponding open-pollinated cones, which ranged from 2.5% to 3.7% (mean=3.0%). However, self-pollinated seeds showed a significantly lower thousand kernel weight (4.26–7.69 g) and germination rate (4.5–17.7%) compared to open-pollinated seeds (4.84–8.59 g and 14.3–33.3%, respectively) (Fig. 2). Self-pollinated seeds also displayed a significantly lower seed soundness (42–64%) compared to open-pollinated seeds (49% to 78%), except for in parent cx569. Self-pollinated seeds presented a significantly higher embryo abortion rate (68.4–91.2%) in comparison with open-pollinated seeds (38.4–78.7%). Intriguingly, the average germination rate (17.7%) of cx569 self-pollinated seeds was higher than those of the self-pollinated seeds from the other five parents. Moreover, the embryo abortion rate of cx569 self-pollinated seeds was lower than that of the self-pollinated seeds of the other five parents. It was found that the cx569 self-pollinated family consistently expressed good growth vigor compared to open-pollinated seeds (up to 14 days old). We assumed that cx569 self-pollinated family (abbreviated as S569) may existed different levels in seedling growth vigor at different growth stages.

cx569 selfed family harbors extremely AD and DE variants at the seedling stage

To test above hypothesis, we continuously observed the growth vigor of cx569 self-pollinated family at seedling stage. The vigor of the 3-month-old self-pollinated family of cx569 appeared to be equal to that of the open-pollinated family. Interestingly, when the seedlings reached 5 months old, the growth of the self-pollinated family of cx569 seemed to significantly exceed the growth of the open-pollinated seedlings (Fig. 3). These results indicated that the S569 showed an absence of inbreeding depression in seedling growth vigor and had different levels of seedling growth vigor. To verify whether there was rarely advanced phenomenon for selfing in S569, we quantified the growth vigor of these seedling populations (5-month-old, n=210) based on the traits of seedling H (Fig. S1). The seedling H of 96 out of 210 seedlings was higher than the mean seedling H of population (6.0 cm). These seedling with highest seedling H (15 cm) is one-fold higher than the seedling with mean seedling H (6.0 cm). However, although there were 111 seedlings that were lower than the mean seedling H, the lowest seedling height of these seedlings was only 3 cm lower than the mean seedling H. These results implied that the rarely advanced phenomenon for selfing was observed in S569. Thus, there exist AD (higher growth vigor) and DE (lower growth vigor) variants in S569 at 5 months old. To reduce the error in the selection of AD and DE variants, three AD variants (seedlings A1, A2, and A3) from the top 50 seedlings with the highest seedling height and three DE variants (seedlings D1, D2, and D3) from the bottom 50 seedlings with the lowest seedling height were selected by using the random function of Microsoft Excel. The three AD variants had a consistent phenotypic morphology. The three different depressed variants included: 1) dwarf, weak, chlorotic, and subsequently withered seedling (seedling D1); 2) dwarf, stunted, no visible pests or diseases, reddish, and leathery seedling (seedling D2); and 3) Seedling D3, similar to seedling D2 in phenotypic characteristics but with normal root growth (Fig. 3B).

Fig. 3. Comparison of growth traits between advanced (AD) and depressed (DE) variants from the cx569 selfed family (5 months old). (A) Height comparison of the self- and open-pollinated family of cx569 in different stages. The data are shown as means ± standard deviation (SD). Student's t-test was used to test for statistical significance (*$P < 0.05$; ns, not significant) between the self-pollinated family and the open-pollinated family in parent cx569. (B) Phenotypic characterization of the cx569 selfed family including three depressed variants (D1, D2, and D3) and three advanced variants (A1, A2, and A3). (C)–(H) Seeding height (H), length of the longest root (LLR), number of roots (RN), fresh weight of seedlings (FWS), fresh weight of the aboveground part (leaves and stem) (FWSL), and fresh weight of the root (FWR), respectively, between AD and DE variants of the cx569 selfed family

The seedling height (H) (13–15 cm) of AD variants was 2-fold higher than that of the DEs. Furthermore, the FWSL and FWS values of ADs were consistently much higher than those in DE plantlets by 16-fold. Similarly, the FWR of ADs was significantly higher than that in DEs by 13-fold. Additionally, the LLR and the RN of ADs appeared to be extremely higher than in DE seedlings. These results suggest that there is a marked difference in morphological index between AD and DE variants.

Transcriptional profiling and gene annotation

In the next step, we conducted a transcriptional profiling assay by RNA-Seq aiming to capture possible genes responsible for the advance growth traits in "S569". In parallel sequencing by RNA-Seq yield, a total of 51.01 Gb clean data and 83,743 unigenes were identified with a high-quality base ratio (Q30) (92.46–93.58%; mean=93.22%) (Table 1). The mean mapped reads value reached 21,764,318, while the mean mapped ratio value reached 76.60%. The GC (guanine-cytosine) content of the reads ranged from 44.33% to 44.81% (mean=44.65%).

To obtain annotation information, the unigenes were annotated into the Nr, Swiss-Prot, GO, COG, KOG, KEGG, and Pfam databases (Table S1). In total, 34,908 unigenes were annotated in the above databases, which accounted for approximately 41.68% of the total unigenes (83,743). Around 39.94% (33,447) of unigenes were detected in the Nr database. About 22.80%, 7.87%, 27.95%, 23.21%, 11.29%, and 19.83% of the unigenes were found in the GO, KEGG, Pfam, Swiss-Prot, COG, and KOG databases, respectively.

As expected, the AD variants (A1, A2, and A3) had close transcriptional relationships with each other ($r^2 > 0.922$), indicating a genetic convergence in germplasms (Fig. 4A). The DE variants (D1, D2, and D3) has moderate correlation with the AD individuals in the transcriptional aspect (r^2 = 0.796–0.863). Moreover, the DE variants displayed small divergence

Table 1. Summary of assembly statistics for the tested samples. Abbreviations: G, guanine; C, cytosine; Q quality score

Variants	Total bases	Read Count	GC (%)	Mapped Reads	Mapped Ratio (%)	Q30 (%)
A1	8,724,002,472	29,121,196	44.81	22,754,108	78.14	92.46
A2	8,058,846,526	26,913,604	44.71	20,913,637	77.71	93.07
A3	9,729,319,038	32,502,309	44.74	25,444,372	78.28	93.35
D1	8,956,414,992	29,942,857	44.64	21,781,963	72.75	93.58
D2	7,345,758,404	24,575,509	44.64	18,804,417	76.52	93.48
D3	8,194,704,274	27,388,246	44.33	20,887,408	76.26	93.35
Average	8,501,507,618	28,407,287	44.65	21,764,318	76.61	93.22

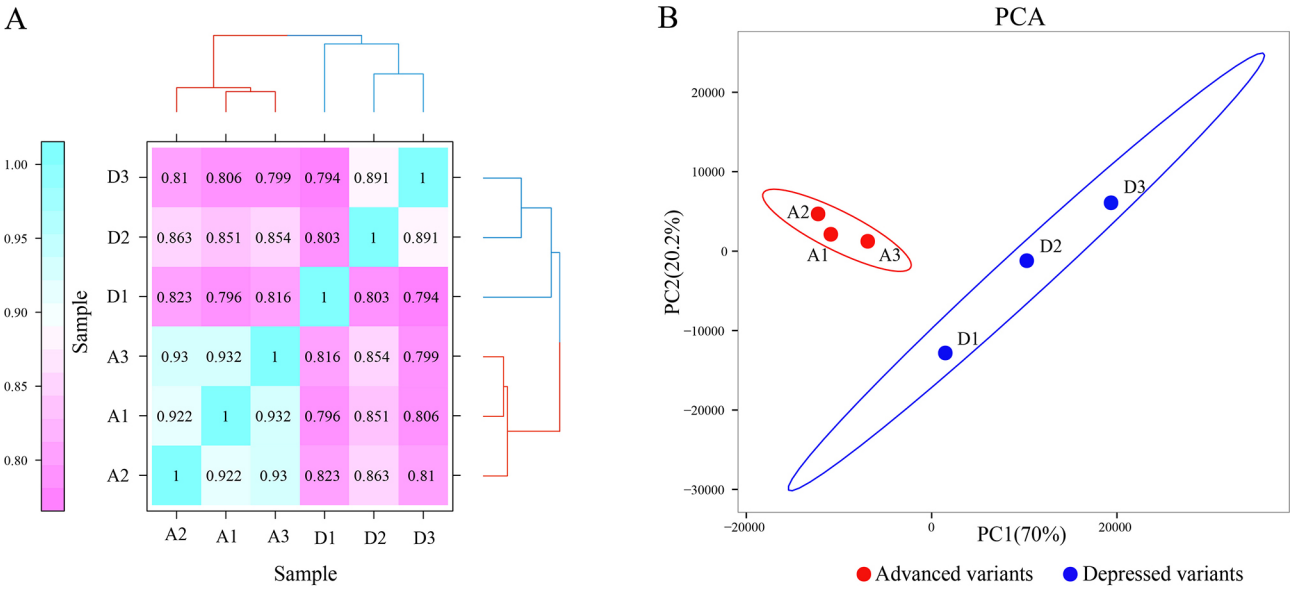

Fig. 4. Correlation between different samples. (A) Cluster dendrogram of different samples based on Spearman's correlation. The red tree line indicates a group of advanced variants (A1, A2, and A3) belonging to the same cluster. The blue tree line refers the same cluster from depressed variants (D1, D2, and D3). The color scale (purple to blue) indicates correlation between samples. The closer r^2 is to 1, the stronger the correlation is between the two samples. (B) Principal component analysis (PCA) of the gene expression data. The red circle indicates a group of elite variants that belong to the same cluster. The blue circle refers to depressed variants belonging to the same cluster

in the transcriptional profiles, presenting correlation coefficients ranging from 0.794 to 0.891. The results of Spearman's correlation analysis indicate that the samples can be divided into two type variants (AD and DE). Principal component analysis (PCA) results also highly agreed with the results of Spearman's correlation analysis, and divided the samples into two clusters (Fig. 4B). Collectively, the samples, with two distinct transcriptome patterns, could be used to identify DEGs in different comparison groups (AD versus DE).

Identification of the deferentially expressed genes between AD and DE

To identify the DEGs between the AD and DE variants, we divided these variants into three comparison groups, and each group consisted of three pairwise comparisons: group I (A1 vs. D1, A2 vs. D1, and A3 vs. D1), group II (A1 vs. D2, A2 vs. D2, and A3 vs. D2), and group III (A1 vs. D3, A2 vs. D3, and A3 vs. D3). Venn diagrams of DEG sets revealed a total of 5450, 5181, and 5517 DEGs in group I, group II, and group III, respectively. In group I, 824 upregulated DEGs belonged to the overlapping set (Fig. 5), while 1473 and 1025 upregulated DEGs belonging to an overlapping set were detected in group II and group III, respectively. In comparison to upregulated DEGs, there were 945, 350, and 964 downregulated DEGs belonging to overlapping sets in group I, group II, and group III, respectively.

Co-expressed genes related to seedling growth traits

The WGCNA captured gene sets related to growth traits (H, FWS, FWLS, FWR, LLR, NR) based on all unigenes (83,743) and phenotypic data. Twenty expression modules of WGCNA were found herein that contained highly interconnected gene clusters with high correlation coefficients between the genes in the same cluster (Fig. 6). Each module harbored positively and negatively correlated genes, and the expression level changed between different morphological traits. Three modules (MEhoneydew1, MElavenderblush3, and MEorangered3) were closely connected

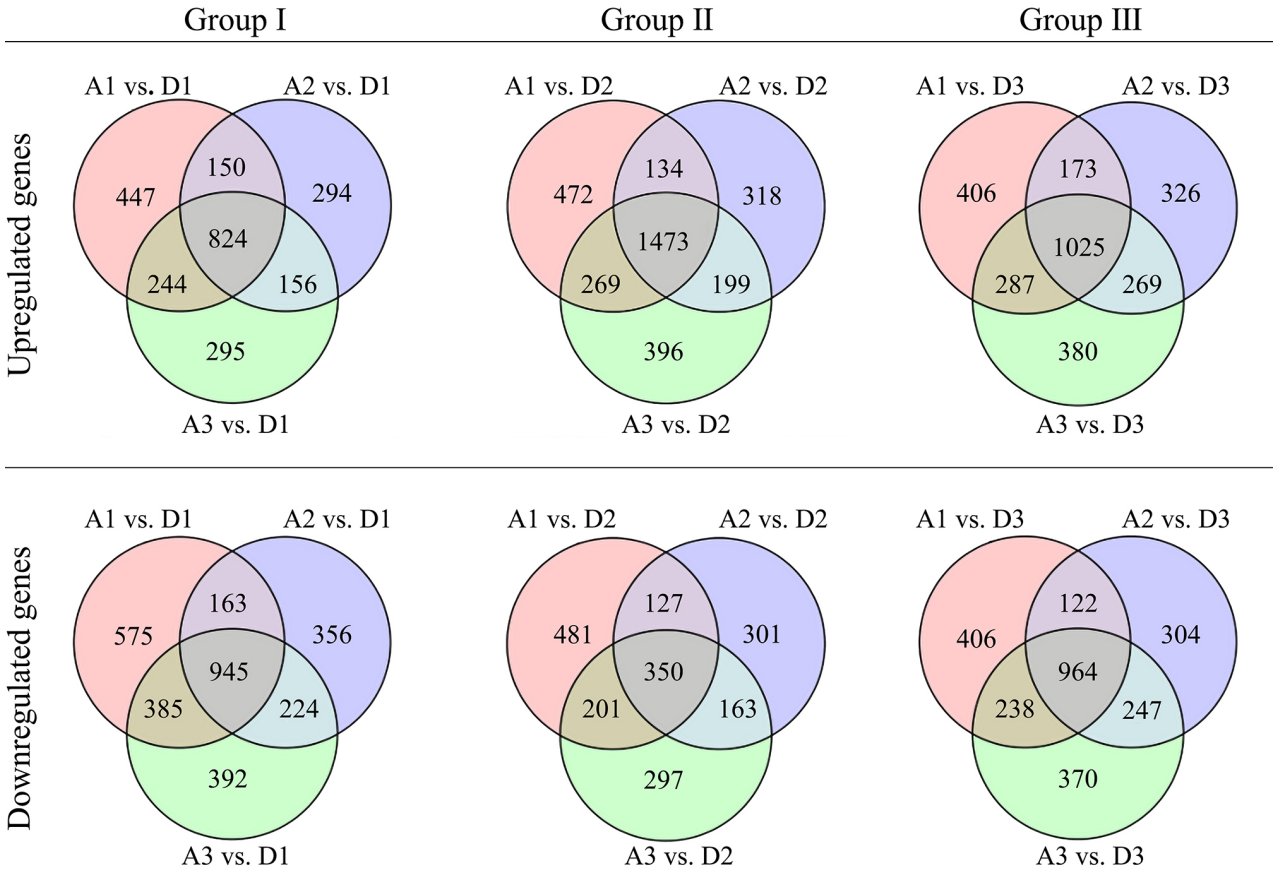

Fig. 5. Venn diagram showing the number of differentially expressed genes (DEGs) between advanced (AD) and depressed (DE) selfing variants. The cut-off value of $\log_2$FC (fold change) > |1| and false discovery rate (FDR) < 0.01. (A) Venn diagrams presenting the upregulated DEGs among three different groups (group I comprises A1 vs. D1, A2 vs. D1, and A3 vs. D1; group II comprises A1 vs. D2, A2 vs. D2, and A3 vs. D2; and group III comprises A1 vs. D3, A2 vs. D3, and A3 vs. D3). (B) Venn diagrams presenting the downregulated DEGs among three different groups

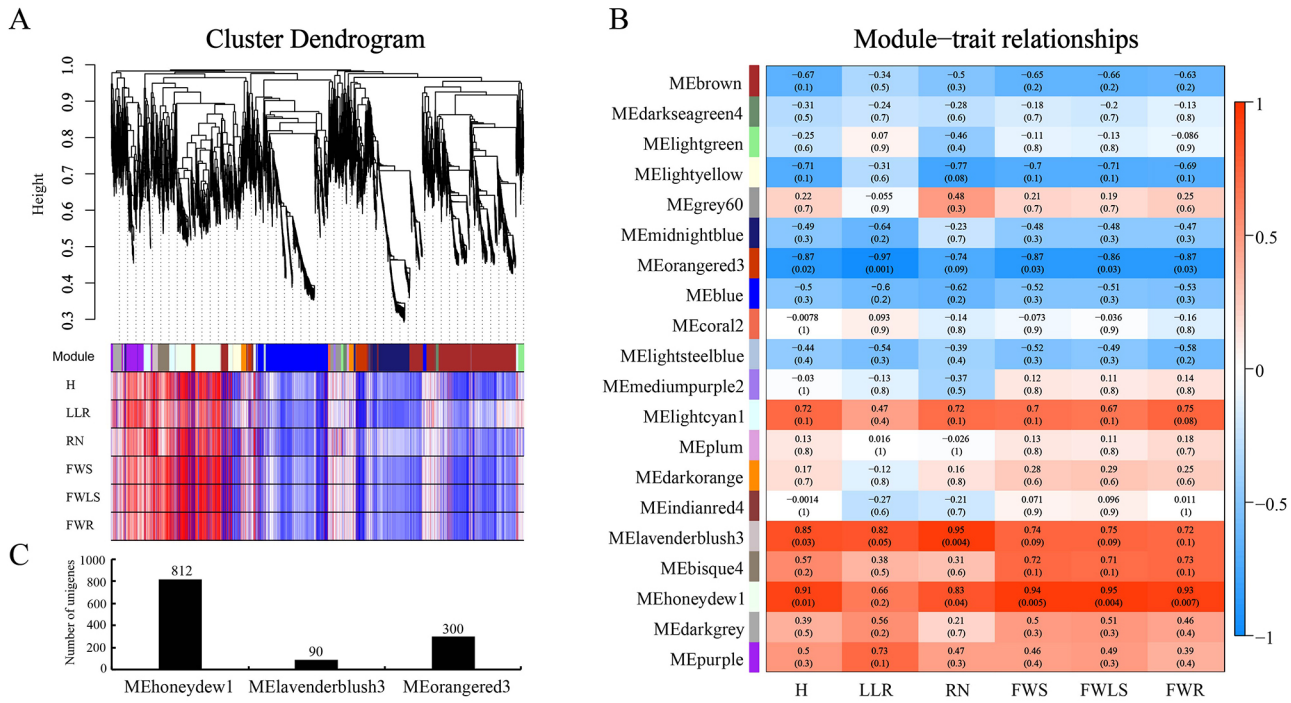

Fig. 6. Weighted gene co-expression network analysis (WGCNA) of all unigenes and module-trait relationships (MTRs) in tested variants. (A) Hierarchical cluster tree presenting 20 modules of co-expressed mRNAs. The intermediate panel provides the modules in distinct colors. The bottom panel shows the correlation between the genes of each trait-related sample and its module. The darker the red color, the greater the positive correlation. In contrast, blue represents negative correlation. (B) Relationships between modules (left) and traits (bottom) in tested samples. (C) The number of unigenes in three significant modules ($p < 0.05$). Red and blue represent positive and negative correlations, respectively. The darker colors suggest higher correlation coefficients. The Pearson's correlation coefficient r^2 values and the *P*-value for each correlation are provided in brackets

with the morphological traits ($r^2 > 0.7$ and $P < 0.05$), expect for LLR growth trait. MEhoneydew1 (r^2=0.91, P=0.01) displayed a remarkably significant positive correlation with H, FWS, FWLS, and FWR (r^2=0.91, P=0.01; r^2=0.94, P=0.005; r^2=0.95, P=0.004; and r^2=0.93, P=0.007, respectively). Moreover, some modules showed a high correlation with the growth traits. For instance, MElavenderblush3 (r^2=0.85, P=0.03) presented a significant positive correlation with H. MEorangered3 (r^2= −0.87, P=0.02) showed a dramatically high negative correlation with H. In addition, the numbers of unigenes in MEhoneydew1 (812) were higher than in MElavenderblush3 (90) and MEorangered3 (300). These results demonstrated that the genes belonging to the three modules were significantly associated with growth traits.

Enrichment analyses

To reveal the specific functions of each co-expressed module, we performed KEGG analysis of unigenes from the MEhoneydew1, MElavenderblush3, and MEorangered3 modules separately (Fig. S2). The biological functions of genes in the MEhoneydew1 module were related to the 'starch and sucrose metabolism', 'phenylalanine metabolism', 'fatty acid elongation', and 'cutin, suberine and wax biosynthesis' pathways, which might have been involved in the selfing seedling growth. The annotation of genes in the MElavenderblush3 module were involved in the 'purine metabolism', 'plant-pathogen interaction', and 'plant hormone signal transduction' pathways. Pathways related to 'phenylpropanoid biosynthesis', 'phenylalanine metabolism', and 'plant hormone signal transduction' were mainly identified for genes in the MEorangered3 module. To identify DEGs in these three modules, we took the overlapped DEGs between groups (group I, group II, and group III) and modules (MEhoneydew1, MElavenderblush3, and MEorangered3), and found that there were 152, 81, and 168 DEGs for significant ($p < 0.05$) modules corresponding to group I, group II, and group III, respectively (Fig. S3). The identified 152 DEGs comprised 12 and 65 annotated DEGs with upregulated and downregulated patterns, respectively, while the other 18 upregulations and 57 downregulations were not annotated. The second identified set (81 DEGs) harbored 16 upregulated and 21 downregulated annotated DEGs, and 27 upregulations and 17 downregulations were not annotated. Among the 168 DEGs for group III, there were 7 upregulations and 77 downregulations with annotated information, while

the other 12 and 72 unknown DEGs displayed upregulated and downregulated patterns, respectively. The identified 152 DEGs for group I comprised 118, 4, and 30 DEGs that fell within the WGCNA modules MEhoneydew1, MElavenderblush3, and MEorangered3, respectively (Table S2). For the second set (81 DEGs), there were 36, 2, and 43 DEGs corresponding to MEhoneydew1, MElavenderblush3, and MEorangered3, respectively. The third set of 168 DEGs harbored 147, 2, and 19 DEGs for MEhoneydew1, MElavenderblush3, and MEorangered3, respectively.

The above overlapped DEGs were then used for enrichment analysis to reveal the biological processes of growth and development responsible for AD and DE variants. The GO enrichment results proved that the involved DEGs of different groups with same modules comprised highly similar GO terms (e.g., biological process, cellular component, and molecular function) (Fig. S4). The KEGG pathway enrichment analysis was also used to identify molecular features with biological roles related to the advanced phenomenon for selfing (Fig. S5). The results of KEGG enrichment revealed that these overlapped DEGs of different groups with the same modules possessed the same critical pathways. In MEhoneydew1, the phenylalanine metabolism, phenylpropanoid biosynthesis, starch and sucrose metabolism, plant-pathogen interaction, cutin and suberine, and wax biosynthesis pathways were all shared in different groups. In MElavenderblush3, different groups embraced similar pathways (e.g., plant hormone signal transduction and nitrogen metabolism pathways). For MEorangered3, the phenylalanine metabolism pathway was found to be shared in both group I and group II. These results showed that the groups and modules identified here were biologically reasonable.

Expression of the hub genes related to growth traits

Heatmaps analyses unraveled the expression level of the overlapped DEGs belonging to the above-mentioned pathways in different groups (Fig. 7). These enriched pathways could relate to the growth and development of AD and were divided into six categories referring to xylem metabolism, sugar and energy metabolism, plant hormone signal transduction, stress response and cytochrome, and transcription factors. Among these overlapped DEGs, 22, 6, and 24 transcription factors (TFs) were detected in groups I, II, and III, respectively. These TFs were mainly represented by the WRKY, ERF, MYB-related, and bHLH families. In addition, the families of the overlapped DEGs associated with xylem metabolism, sugar and energy metabolism, plant hormone signal transduction, stress response, and cytochrome in the three groups were also extremely similar. The expression level of xylem metabolism-related, sugar and energy metabolism-related, and plant hormone signal transduction-related genes showed overrepresented expression in the AD variants, while the expression levels of the majority of stress response-related genes exhibited high expression in the DE variants. However, these overlapped DEGs exhibited similar expression levels in different groups.

Twenty-three important overlapped DEGs consistently expressed in pairwise comparisons were specifically focused on in the next step (Table S3). These 23 overlapped DEGs were mainly involved in encoding xylem metabolism (*PER3*, *LAC4*, *CESA8*, and *CESA9*), plant hormone signal transduction (*GID1* and *GAMT2*), stress response (*PR1, PR10,* and *TIR/NBS/LRR*), sugar and energy metabolism-related (*GMPP* and *NRT*), and cytochrome (*CYP707A1, CYP716B1, CYP76B10, CYP77A1, CYP77A3, CYP82C4, CYP86B1, and CYP86B1-2*), in addition to transcription factor aspects (*WRKY6*, *WRKY31*, *ERF071*, and *MYB-related 305*). In terms of gene expression level (FPKM values), *MYB-related 305*, *PER3*, *LAC4*, *CESA8*, *CESA9*, *GID1*, *CYP77A1*, *CYP77A3*, *CYP86B1*, *CYP86B1-2*, *GMPP*, and *NRT* genes were all expressed at moderately high levels in AD variants (11.1–46.8 FPKM) compared to DE variants with a extend change by 3.6–65.9 folds. In the meantime, the FPKM values of *CYP707A1*, *CYP82C4*, *GAMT2*, and *TIR/NBS/LRR* genes reached over 5.9–fold (5.9– to 42.9–fold) in AD variants (4.2–6.2 FPKM) in comparsion with DE variants. In the field of *ERF071*, *WRKY6*, *WRKY31*, *PR1*, *YP76B10*, *CYP716B1*, and *PR10* genes, the expression values of the AD variants (0.2–3.0 FPKM) were significantly lower than those of the DE variants (4.0–37.3 FPKM), which were only 5.7% to 18.0%.

Deduced network and pathway responsible for the advanced AD growth traits

In order to further explore the key genes in cx569 selfed family associated with rarely advanced phenomenon, the pairs of DEGs with the absolute value of correlation coefficient greater than 0.8 in comparison group I, group II, and group III were screened. Then the degree (the number of connections between a gene and other genes in the regulatory network) of the pairs of DEGs were calculated by Cytoscape software. The DEGs with the degree of top ten and the correlation coefficient greater than 0.9 were preferentially selected. Precisely these ten DEGs (*PER3*, *LAC4*, *CESA8*, *CESA9*, *GID1*, *PR1*, *WRKY6*, *WRKY31*, *ERF071*, and *MYB-related 305*) overlapped with the above twenty-three important DEGs were

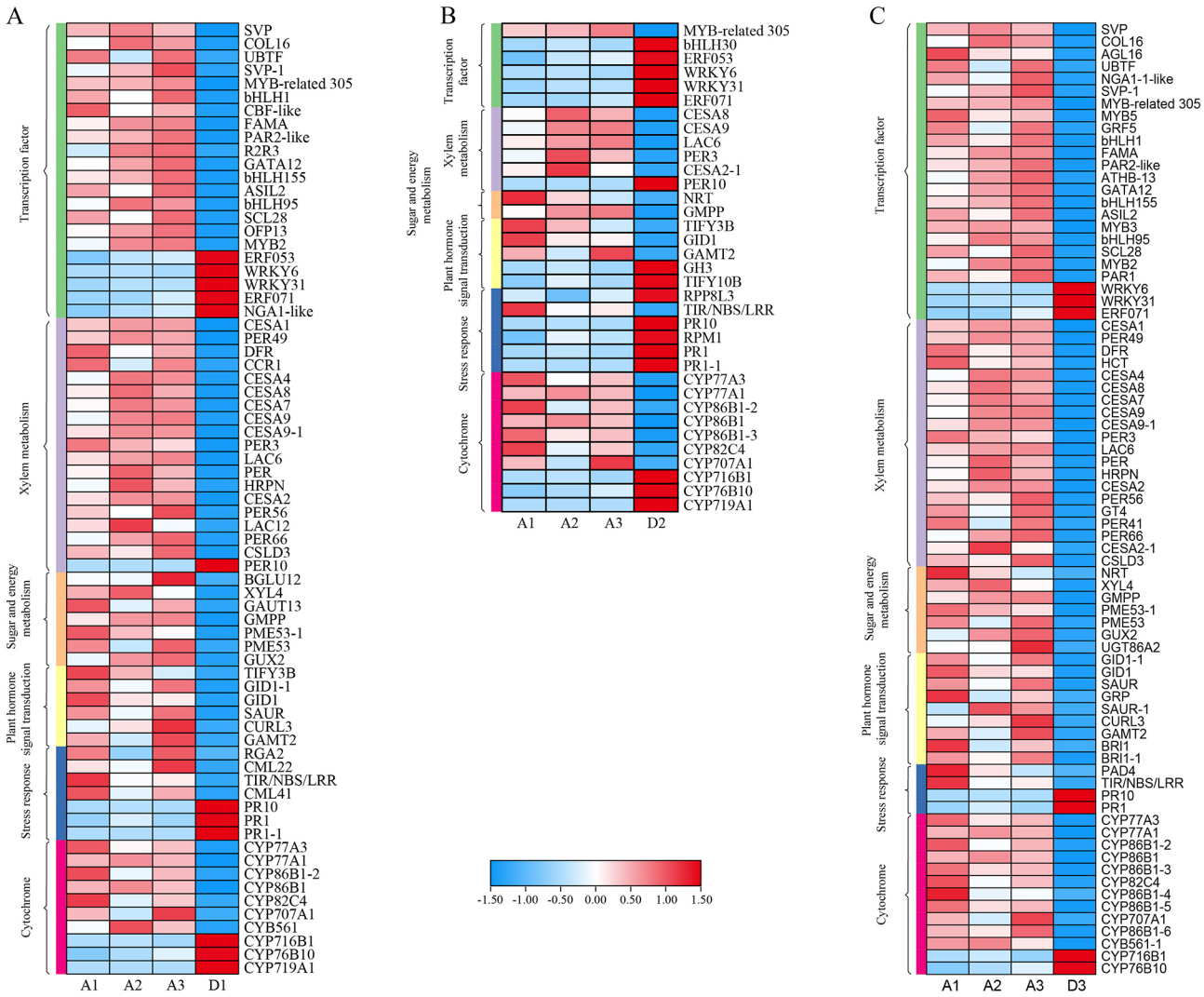

Fig. 7. Heatmaps showing the transcriptomic profiles of the differentially expressed genes (DEGs) related to potentially controlling the growth and development of selfing variants in group I (A), group II (B), and group III (C) using normalized $\log_2$ expression data (FPKM). The blue bands indicate low gene expression quantity, and the red bands indicate high expression quantity

regarded as hub genes. These ten hub genes may be played a key role in selfed family growth which had advanced phenomenon. The three deduced networks were constructed using the above hub genes and other genes to address the relationships between genes, which were based on gene pairs for an absolute value of correlation coefficient >0.8 (Fig. 8). The reactions between the hub genes and the other genes in the corresponding network may be responsible for AD growth and development. These genes were mainly divided into six types: xylem metabolism-related, sugar and energy metabolism-related, plant hormone signal transduction-related, stress response-related, cytochrome-related, and transcription factor genes. The xylem metabolism-related and plant hormone signal transduction-related genes exhibited more relationships with other genes in different groups. In addition, the number of gene pairs in group I and group III with positive correlations (1224 and 1815, respectively) was higher than that of genes with negative correlations (657 and 449, respectively), while group II exhibited fewer gene pairs with positive correlations (209) compared to gene pairs with negative correlations (263). These results indicate that there may be similar regulation networks for AD variants.

The KEGG pathways analyses revealed that phenylpropanoid biosynthesis, phenylalanine metabolism, and plant hormone signal transduction were the most enriched pathways (Fig. S5). These hub genes may affect the growth of variants by being involved in several important synthetic and metabolic pathways. For instance, the *PER3* and *LAC4* genes in the AD variants presented upregulation in the lignin biosynthetic pathway, whereas the *PR1* gene in the AD variants showed downregulation in plant hormone

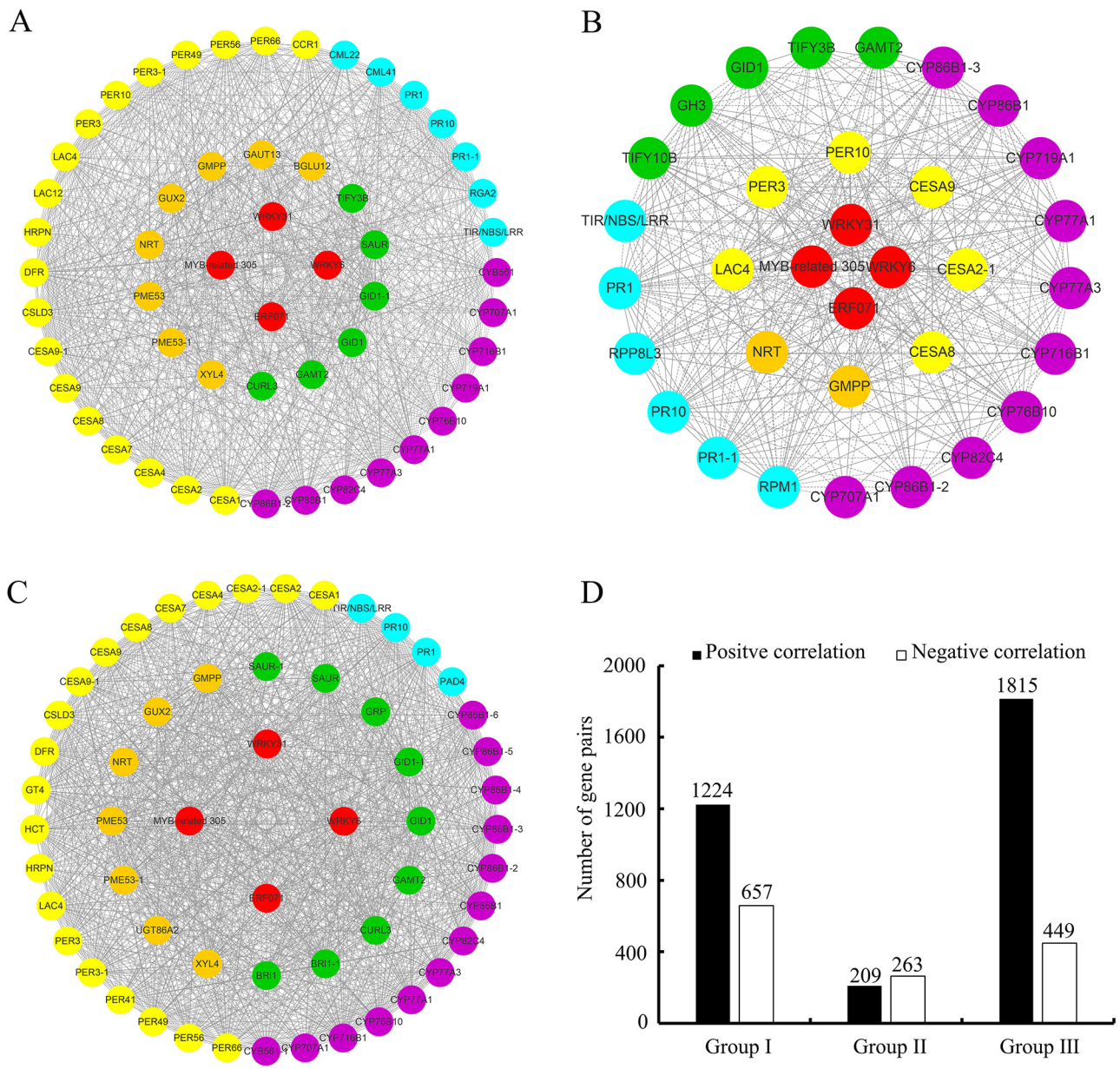

Fig. 8. Co-expression gene networks based on correlation coefficient > 0.8 in different groups. Overlapped differentially expressed genes (DEGs) selected from three significant ($p < 0.05$) modules (MEhoneydew1, MElavenderblush3, and MEorangered3) corresponding to group I, group II, and group III. Red circular nodes indicate transcription factors, orange circular nodes indicate sugar and energy metabolism-related genes, green circular nodes indicate plant hormone signal transduction-related genes, yellow circular nodes indicate xylem metabolism-related genes, blue circular nodes indicate stress response-related genes, and purple circular nodes indicate cytochrome-related genes. Solid lines indicate positive correlations and dashed lines represent negative correlations. (A) Co-expression gene network constructed by DEGs from group I and the three modules. (B) Co-expression gene network constructed by DEGs from group II and the three modules. (C) Co-expression gene network constructed by DEGs from group III and the three modules. (D) The number of gene pairs with an absolute value of correlation coefficient > 0.8 in three co-expression gene networks

signal transduction (Fig. 9). Furthermore, the *GID1* and *CESA8* (or *CESA9* gene) genes from AD variants were upregulated in the plant hormone signal transduction and the cellulose biosynthetic pathway, respectively. The gene expression profiling of hub genes in the above pathways implied significant differences in the growth and development of AD and DE variants. In a nutshell, these hub genes, which mainly encoded various proteins involved in complex plant hormone-mediated signaling pathways, led to the different expression levels in AD and DE variants and further implied that the 10 hub genes were largely responsible for the advanced growth traits of AD variants.

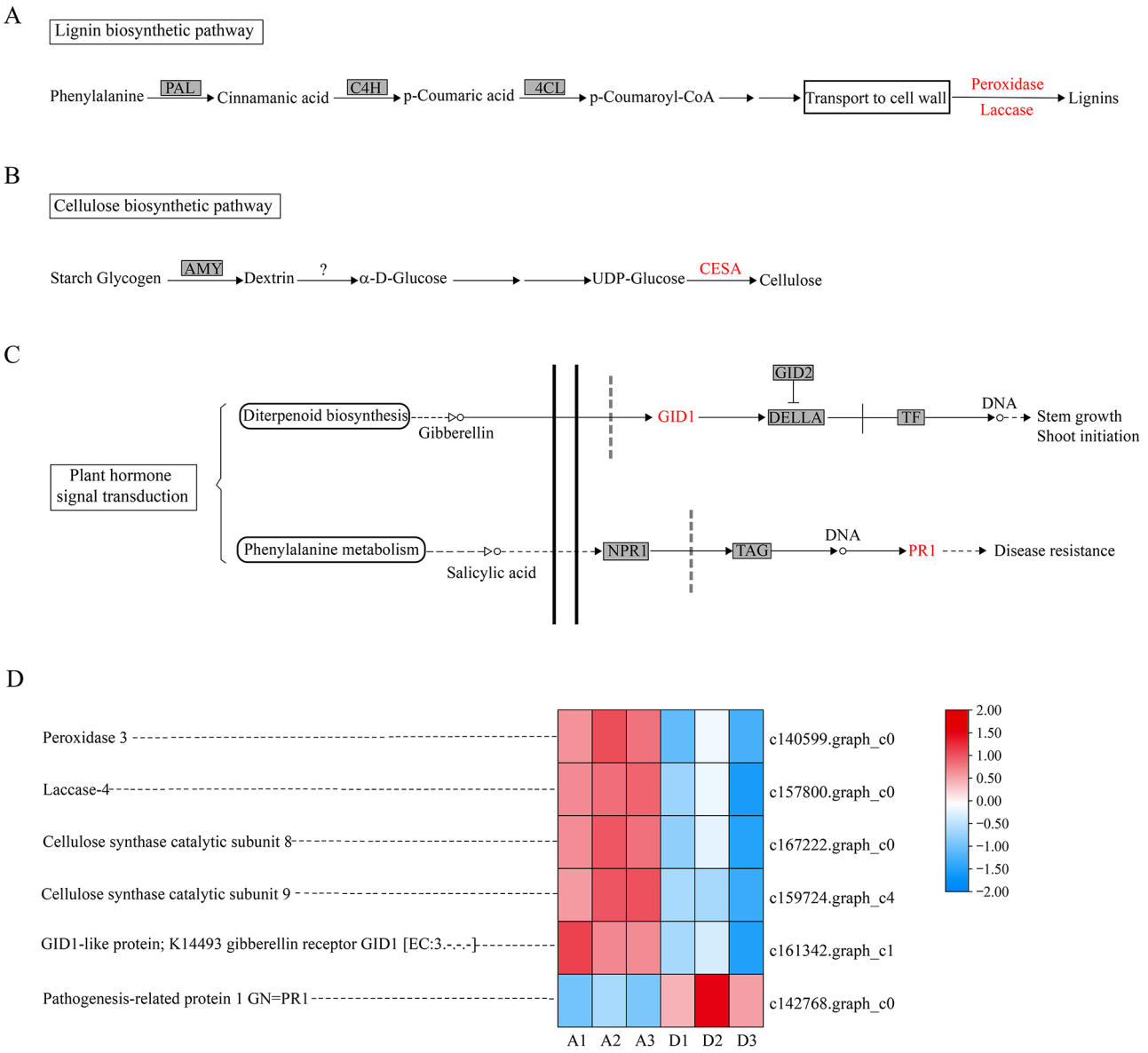

Fig. 9. The pathway showing the hub genes involved the key nodes related to plant growth. The hub genes that may be involved in the lignin biosynthetic pathway, cellulose biosynthetic pathway, and plant hormone signal transduction pathway are shown in figures (A)–(C), respectively. (D) Heatmaps of hub genes using normalized $\log_2$ expression data (FPKM). The blue bands indicate low gene expression quantity, and the red bands indicate high expression quantity

Discussion

Transcriptome analysis has revealed that the growth and development of selfed progeny involves the interaction of multiple genes and pathways (Arro et al., 2017). Network-based dependency analysis further revealed that most of the significantly rewired connections among the ten most connected hub genes (e.g., *PRX52*) involved at least one transcription factor (e.g., *TCP3*), and these hub genes played a key role in development of selfed progeny (Arro et al., 2017). Herein, we performed a comparative RNA-Seq analysis to identify genes associated with seedling advance growth traits in a special selfed family termed as S569 in Chinese fir. Ten hub genes with high correlation coefficients (greater than 0.9), including *WRKY6*, *WRKY31*, *ERF071*, *MYB-related 305*, *PER3*, *LAC4*, *CESA8*, *CESA9*, *GID1*, and *PR1*, were detected in each pairwise comparison of AD and DE variants. These hub genes were involved in pathways related to transcription factors, xylem metabolism, plant hormone signal transduction, and stress response. Furthermore, the hub gene-linked interaction networks and pathways uncovered herein may be responsible for the unusually advanced phenomenon for selfing at the seedling stage of Chinese fir.

Inbreeding depression is prevalent in plant kingdoms and may be caused by the exposure of

deleterious alleles and/or loss of overdominant alleles resulting from increased homozygosity, or reduced recombination frequency in some regions (Charlesworth & Willis, 2009; McMullen et al., 2009; Zhang et al., 2019). However, the distinct alleles that are present in a genotype are assumed to be known, but not the frequency with which they occur (Ridout et al., 2001). Furthermore, higher heterozygous were detected in genomes of selfed offsprings of a single parent tree (*Eucalyptus grandis*), and although high inbreeding depression was observed in these offsprings resulting from pseudo-overdominace, heterozygote advantage could not be excluded (Hedrick et al., 2016). Therefore, due to the recombination of alleles, the selfed progeny may show different inbreeding depression. Evidence has also confirmed an increase in within-family variance with increasing inbreeding in conifers (Sniezko & Zobel, 1988; Matheson et al., 1995; Wu et al., 1998). In this study, we found different levels of variance in the selfed families of different parents and observed good performance in S569 at seedling stage. This finding is consistent with our hypothesis on AD and DE variants are observed from S569 during seedling development stage. Moreover, inbreeding depression for juvenile height growth is relatively smaller in western redcedar than that reported in other conifers (Wang & Russell, 2006). Dong et al. (2020) discovered that selfed progeny did not show severe inbreeding depression for survival or growth in Japanese larch (*Larix kaempferi*). These results indicate that an absence of inbreeding depression for growth may occur in specific individuals in wild plants. However, most growth traits in plants are quantitative traits controlled by numerous genes. Genes that control quantitative traits are more likely to form co-expression networks than other genes expressed in organs (Zhang et al., 2020). Therefore, the interaction of multiple genes and pathways may be responsible for S569 showing the positive effect in seedling stage.

Transcription factors play an important key role in plant growth and development (Chen et al., 2021). In this study, a set of TFs were identified between AD and DE variants. It should be noted that the four hub TFs (*MYB-related 305*, *ERF071*, *WRKY6*, and *WRKY31*) are shared in each pairwise comparison. MYB-related proteins were found to control the expression of phenylpropanoid metabolism from phenylalanine, and the first enzyme of phenylpropanoid metabolism, phenylalanine ammonia lyase, was encoded by a gene activated by *AmMYB305* (Martin & Paz-Ares, 1997). Moreover, some *MYB* genes serve roles in controlling the branch of phenylpropanoid metabolism involved in lignin production due to their high expression in tissues such as differentiating xylem (Campbell et al., 1995). In this study, the *MYB-related 305* gene was upregulated in elite variants. This indicates that the *MYB-related 305* gene may be a suitable candidate gene for mediating the expression of the gene responsible for the advanced phenomenon for selfing in Chinese fir seedlings. The APETALA2/ETHYLENE RESPONSIVE FACTOR (*AP2/ERF*) family TFs (*AP2/ERFs*) are key regulators of plant growth and various stress responses. They also respond to hormones and induce improved plant survival under various stress conditions (Xie et al., 2019). Evidence has confirmed that photosynthesis is suppressed by the *ERF071* gene in *Oryza sativa* (Ahn et al., 2017). Our comparative transcriptome data reveal that the *ERF071* gene was significantly upregulated in DE variants, which further suggested that the growth of depressed seedlings may have been inhibited by photosynthesis. Most *WRKY* transcription factors help to defend plants against phytopathogens and abiotic and biotic stresses in many plant species (Robatzek & Somssich, 2002; Zheng et al., 2007; Birkenbihl et al., 2017; Jia et al., 2021; Yao et al., 2020; Zhang et al., 2021; Jiang et al., 2021). In particular, Skibbe et al. (2008) identified a crucial role of *WRKY3* and *WRKY6* in enhancing and/or sustaining active jasmonic acid (JA) levels during continuous insect attack. In addition, the overexpression of *GmWRKY31* in transgenic soybean potentiated resistance to *Phytophthora sojae* by regulating *GmNPR1* (Fan et al., 2017). These results indicate that the *WRKY*-type genes (such as *WRKY6* and *WRKY31*) in many plant species are mainly involved in responses to phytopathogens and abiotic and biotic stresses. In our report, the upregulation of *WRKY6* and WRKY*31* in DE variants may be involved in plant-pathogen interactions and stress responses.

Lignin is a complex phenolic polymer that exists in the secondary cell walls of all vascular plants (Zhao, 2016). Lignin provides structural rigidity that allows tracheophytes to stand upright, and potentiates the cell wall to withstand the negative pressure generated during transpiration (Weng & Chapple, 2010). The currently accepted lignin biosynthetic partial pathway in plants is shown in **Fig. 9A** (Zhao, 2016). Peroxidase (*PER*) and laccase (*LAC*) genes are the two key candidates for lignin polymerization. Schuetz et al. (2014) reported that the precise transport and deposition of monolignols were guided by lignin laccases. Studies showed that the loss of function of LACCASE4 (*LAC4*), *LAC11*, and *LAC17* genes in *Arabidopsis* had a significant effect on the lignification of metaxylem and fiber cells in inflorescence stems (Berthet et al., 2011; Zhao et al., 2013). It has also been argued that lignin polymerization activity originated from peroxidase genes because the peroxidase genes expanded significantly in association with the rise of vascular plants (Weng & Chapple, 2010). Herein, the expression of the *LAC4* and *PER3*

genes was higher in elite variants compared to DE variants, which may have been the reason that AD variants harbored elite traits (e.g., seedling height) (Fig. 3C and Fig. 9D). Additionally, cellulose is the main chemical component of the plant cell secondary wall, and is dramatically related to wood quality (Huang et al., 2012). Based on previous studies, a hypothetical partial pathway of cellulose biosynthesis is presented in Fig. 9B (Kimura & Kondo, 2002; Huang et al., 2012; Lyu et al., 2020). Recently, analysis in *A. thaliana* revealed that *AtCesA6*-null mutants presented a reduced cell elongation of young seedlings with little effect on cell division, thus affecting the cellular integrity and biomass yield in mature plants (Hu et al., 2018). However, the co-overexpression of *AtCesA2* and *AtCesA5* in *AtCesA6*-null mutants could significantly promote cell division and completely restore cell wall integrity, resulting in a remarkable increase in secondary wall thickness and biomass production in mature plants (Hu et al., 2018). Interestingly, the average expression of the *LusCesA4* and *LusCesA7* genes is relatively high in flax seedlings and further increases in stems at the rapid growth stage, whereas the average expression of the *LusCesA1* and *LusCesA6* genes decreases (Galinousky et al., 2019). Furthermore, functional cellulose synthesis complexes (CSCs) are composed of at least three different cellulose synthase catalytic subunits (*CESAs*) in *A. thaliana*, and the results of analysis show that *CESA1*, *CESA3*, and *CESA6* are present in a 1:1:1 molecular ratio based on spectral counting (Gonneau et al., 2014). Herein, we identified eight different *CESA* genes in three groups, among which two genes (*CESE8* and *CESA9*) were shared in each pairwise comparison. These two genes were highly expressed in AD variants, which further indicated that the vigorous growth of elite seedlings may have been related to the combined effects of these two genes and other *CESAs*.

It has been shown that genes involved in plant hormone biosynthesis and signaling are associated with plant growth and development (Livne & Weiss, 2014; Verma et al., 2016; Willoughby & Nimchuk, 2021). GIBBERELLIN-INSENSITIVE DWARF1 (*GID1*), as a gibberellin (*GA*) receptor, is an important component of the *GA* signaling pathway (Ueguchi-Tanaka et al., 2007). One study showed that over-expression of each Ta*GID1* gene in the *Arabidopsis* double mutant gid1a/1c partially rescued the dwarf phenotype (Li et al., 2013). Liang et al. (2014) demonstrated that the silencing of the *GID1* genes (*GA* receptor genes) led to stunted growth and dark-green leaves with late flowering in *Petunia*. In addition, the *Arabidopsis* mutant (*gid1a gid1c*) displayed a dwarf phenotype due to the lack of the *GID1* gene, and the triple mutant presented a dwarf phenotype more severe than that of the extreme *GA*-deficient mutant ga1-3 (Griffiths et al., 2006). We identified two unigene sequences annotated as encoding *GID1* genes, among which one *GID1* gene was shared in each pairwise comparison. The expression of the *GID1* gene in AD variants was higher than in DE variants (Fig. 9D). Pathogenesis-related protein 1 (*PR1*) is one of the most abundantly produced proteins in plant defense responses, and is indirectly regulated by salicylic acid to impact plant growth (Breen et al., 2017; Venegas-Molina et al., 2020). Moreover, Lincoln et al. (2018) demonstrated that *PR1* could inhibit cell death in plants, which was consistent with the mode in animals in suppressing cell death-dependent disease symptoms. *PR1* proteins are not completely related to host defense. Numerous reports have shown that *PR1* genes are responsive to abiotic stimuli, indicating that they play important roles in abiotic stress responses (Dixon et al., 1991; Liu et al., 2013; Kothari et al., 2016; Venegas-Molina et al., 2020; Chmielowska-Bąk & Deckert, 2021). In this study, the expression of *PR1* showed a higher expression level in DE than the AD variants', indicating a pre-stress activity in these seedlings (DE variants).

Conclusion

In this study, self-pollination experiments revealed a wide variation in selfing effects among parents. We captured a potentially advanced family (S569) for selfing of Chinese fir expressing elite traits at the seedling stage. The growth-based AD and DE variants were subjected to comparative RNA-Seq analysis with the aim to illustrate the underlying molecular mechanism, especially the hub gene-regulated networks and pathways responsible for the rarely advanced phenomenon for selfing in Chinese fir. In total, the transcriptome data revealed more than 5000 DEGs for each comparison group (AD versus DE). Through WGCNA, 152, 81, and 168 overlapped DEGs were found for significant ($p<0.05$) modules (MEhoneydew1, MElavenderblush3, and MEorangered3) corresponding to three groups (group I, group II, and group III, respectively). These overlapped DEGs harbored similar gene expression patterns in different groups. A subsequent enrichment analysis showed that the identified DEGs belonged to six main types, including xylem metabolism-related, sugar and energy metabolism-related, plant hormone signal transduction-related, stress response-related, cytochrome-related, and transcription factor genes. Ten hub genes represented by the *ERF071*, *MYB-relate 305*, *WRKY6*, *WRKY31*, *PER3*, *LAC4*, *CESA8*, *CESA9*, *GID1*, and *PR1* genes were co-identified between AD and DE variants. This set of hub-gene-linked interaction networks and pathways may be responsible for the

rarely advanced phenomenon for selfing at the seedling stage in Chinese fir. In future research, we will study the influence of these gene interactions on the growth and development of selfed offsprings.

Acknowledgments

This research was supported by the National Natural Science Foundation of China (No. 31972956) and the Key-Area Research and Development Program of Guangdong Province (No. 2020B020215001). We thank Dr. Rong Huang from Southern Medical University in China for paper revision.

References

Ahn H, Jung I, Shin SJ, Park J, Rhee S, Kim JK, Jung W, Kwon HB & Kim S (2017) Transcriptional network analysis reveals drought resistance mechanisms of AP2/ERF transgenic Rice. Frontiers in Plant Science 8: e1044. doi:10.3389/fpls.2017.01044.

Alexa A & Rahnenfuhrer J (2010) topGO: Enrichment analysis for gene ontology. R package version 2: 2010.

Apweiler R, Bairoch A, Wu CH, Barker WC, Boeckmann B, Ferro S, Gasteiger E, Huang HZ, Lopez R, Magrane M, Martin MJ, Natale DA, O'Donovan C, Redaschi N & Yeh LSL (2004) UniProt: the universal protein knowledgebase. Nucleic Acids Research 32: 115–119. doi:10.1093/nar/gkh131.

Arro J, Cuenca J, Yang Y, Liang Z, Cousins P, & Zhong G (2017) A transcriptome analysis of two grapevine populations segregating for tendril phyllotaxy. Horticulture Research 4: e17032. doi:10.1038/hortres.2017.32.

Ashburner M, Ball CA, Blake JA, Botstein D, Butler H, Cherry JM, Davis AP, Dolinski K, Dwight SS, Eppig JT, Harris MA, Hill DP, Issel-Tarver L, Kasarskis A, Lewis S, Matese JC, Richardson JE, Ringwald M, Rubin GM & Sherlock G (2020) Gene ontology: tool for the unification of biology. The Gene Ontology Consortium. Nature Genetics 25: 25–29. doi:doi.org/10.1038/75556.

Barragan AC, Collenberg M, Schwab R, Kerstens M, Bezrukov I, Bemm F, Požárová D, Kolář F & Weigel D (2021) Homozygosity at its Limit: Inbreeding depression in wild *Arabidopsis arenosa* populations. BioRxiv 1: e427284. doi:10.1101/2021.01.24.427284.

Benjamini Y & Hochberg Y (1995) Controlling the false discovery rate: a practical and powerful approach to multiple testing. Journal of the Royal Statistical Society 5: 289–300. doi:10.1111/j.2517-6161.1995.tb02031.x.

Berthet S, Demont-Caulet N, Pollet B, Bidzinski P, Cézard L, Le Bris P, Borrega N, Hervé J, Blondet E, Balzergue S, Lapierre C & Jouanin L (2011) Disruption of LACCASE4 and 17 results in tissue-specific alterations to lignification of *Arabidopsis thaliana* stems. Plant Cell 23: 1124–1137. doi:10.1105/tpc.110.082792.

Birkenbihl RP, Kracher B, Roccaro M & Somssich IE (2017) Induced genome-wide binding of three *Arabidopsis* WRKY transcription factors during early MAMP-triggered immunity. Plant Cell 29: 20–38. doi:10.1105/tpc.16.00681.

Breen S, Williams SJ, Outram M, Kobe B & Solomon PS (2017) Emerging insights into the functions of pathogenesis-related protein 1. Trends Plant Science 22: 871–879. doi:10.1016/j.tplants.2017.06.013.

Campbell MM, Whetten RW & Sederoff RR (1995) Myb homologs in loblolly-pine xylem. Plant Physiology 108: 28.

Charlesworth D & Willis JH (2009) The genetics of inbreeding depression. Nature Reviews Genetics 10: 783–796. doi:10.1038/nrg2664.

Chen Cj, Chen H, Zhang Y, Thomas HR, Frank MH, He YH & Xia R (2020) TBtools: An integrative toolkit developed for interactive analyses of big biological data. Molecular Plant 13: 194–1202. doi:10.1016/j.molp.2020.06.009.

Chen SF, Zhou YQ, Chen YR & Gu J (2018) fastp: an ultra-fast all-in-one FASTQ preprocessor. Bioinformatics 34: 884–890. doi:10.1093/bioinformatics/bty560.

Chen LJ, Wu F & Zhang JY (2021) NAC and MYB families and lignin biosynthesis-related membersidentification and expression analysis in *Melilotus albus*. Plants 10: 303. doi:10.3390/plants10020303.

Chmielowska-Bąk J & Deckert J (2021) Plant recovery after metal stress-a review. Plants 10: 450. doi:10.3390/plants10030450.

Collin CL, Penet L & Shykoff JA (2009) Early inbreeding depression in the sexually polymorphic plant Dianthus sylvestris (*Caryophyllaceae*): Effects of selfing and biparental inbreeding among sex morphs. American Journal of Botany 96: 2279–2287. doi:10.3732/ajb.0900073.

Cornetti L, Fields PD & Ebert D (2021) Genomic characterization of selfing in the cyclic parthenogen *Daphnia magna*. Journal Evolutionary Biology 34: 792–802. doi:10.1111/jeb.13780.

Cronn R, Dolan P C, Jogdeo S, Wegrzyn JL, Neale DB, Clair JBS & Denver DR (2017) Transcription through the eye of a needle: daily and annual cyclic gene expression variation in Douglas-fir needles. BMC Genomics 18: e558. doi:10.1186/s12864-017-3916-y.

Cuénin N, Flores O, Rivière E, Lebreton G, Reynaud B & Martos F (2019) Great genetic diversity but high selfing rates and short-distance gene flow characterize populations of a Tree (*Foetidia*; Le-

cythidaceae) in the fragmented tropical dry forest of the Mascarene Islands. Journal of Heredity 110: 287–299. doi:10.1093/jhered/esy069.

Deng YY, Li JQ, Wu SF, Zhu YP, Chen YW & He FC (2006) Integrated nr database in protein annotation system and its localization. Computations Engineering 32: 71–74.

Del Castillo RF & Trujillo S (2008) Effect of inbreeding depression on outcrossing rates among populations of a tropical pine. New Phytologist 177: 517–524. doi:10.1111/j.1469-8137.2007.02260.x.

Dixon DC, Cutt JR & Klessig DF (1991) Differential targeting of the tobacco PR-1 pathogenesis-related proteins to the extracellular space and vacuoles of crystal idioblasts. The Embo Journal 10: 1317–1324. doi:10.1002/j.1460-2075.1991.tb07650.x.

Dong LM, Xie YH & Sun XM (2020) Full-diallel-based analysis of genetic parameters for growth traits in Japanese larch (*Larix kaempferi*). New Forests 51: 261–271. doi:10.1007/s11056-019-09729-6.

Duan HJ, Cao S, Zheng HQ, Hu DH, Lin J, Cui BB, Lin HZ, Hu RY, Wu B, Sun YH & Li Y (2017) Genetic characterization of Chinese fir from six provinces in southern China and construction of a core collection. Scientific Report 7: e13814. doi:10.1038/s41598-017-13219-0.

Duangjit J, Bohanec B, Chan AP, Town CD & Havey MJ (2013) Transcriptome sequencing to produce SNP-based genetic maps of onion. Theoretical and Applied Genetics 126: 2093–2101. doi:10.1007/s00122-013-2121-x.

Fan SJ, Dong LD, Han D, Zhang F, Wu JJ, Jiang LY, Cheng Q, Li RP, Lu WC, Meng FS, Zhang SZ & Xu PF (2017) GmWRKY31 and GmHDL56 enhances resistance to *Phytophthora sojae* by regulating defense-related gene expression in soybean. Frontiers in Plant Science 8: 781. doi:10.3389/fpls.2017.00781.

Feng XX, Liu S, Cheng HL, Zuo DY, Zhang YP, Wang QL, Lv LM & Song GL (2021) Weighted gene co-expression network analysis reveals hub genes contributing to fuzz development in *Gossypium arboreum*. Genes 12: 753. doi:10.3390/genes12050753.

Finn RD, Bateman A, Clements J, Coggill P, Eberhardt RY, Eddy SR, Heger A, Hetherington K, Holm L, Mistry J, Sonnhammer ELL, Tate J & Punta M (2014) Pfam: the protein families database. Nucleic Acids Research 42: 222–230. doi:10.1093/nar/gkt1223.

Ford GA, McKeand SE, Jett JB & Isik F (2015) Effects of inbreeding on growth and quality traits in Loblolly pine. Forest Science 61: 579–585. doi:10.5849/forsci.13-185.

Galinousky D, Padvitski T, Bayer G, Pirko Y, Pydiura N, Anisimova N, Nikitinskaya T, Khotyleva L, Yemets A, Kilchevsky A & Blume Y (2019) Expression analysis of cellulose synthase and main cytoskeletal protein genes in flax (*Linum usitatissimum L)*. Cell Biology International 43: 1065–1071. doi:10.1002/cbin.10837.

García de la Torre VS, Majorel-Loulergue C, Rigaill GJ, Alfonso-González D, Soubigou-Taconnat L, Pillon Y, Barreau L, Thomine S, Fogliani B, Burtet-Sarramegna V & Merlot S (2021) Wide cross-species RNA-Seq comparison reveals convergent molecular mechanisms involved in nickel hyperaccumulation across dicotyledons. New Phytologist 229: 994–1006. doi:10.1111/nph.16775.

Gonneau M, Desprez T, Guillot A, Vernhettes S & Höfte H (2014) Catalytic subunit stoichiometry within the cellulose synthase complex. Plant Physiology 166: 1709–12. doi:10.1104/pp.114.250159.

Griffiths J, Murase K, Rieu I, Zentella R, Zhang ZL, Powers SJ, Gong F, Phillips AL, Hedden P, Sun TP & Thomas SG (2006) Genetic characterization and functional analysis of the GID1 gibberellin receptors in *Arabidopsis*. The Plant Cell 18: 3399–3414. doi 10.1105/tpc.106.047415.

Haas BJ, Papanicolaou A, Yassour M, Grabherr M, Blood PD, Bowden j, Couger MB, Eccles D, Li B, Lieber M, MacManes MD, Ott M, Orvis J, Pochet N, Strozzi F, Weeks N, Westerman R, William T, Dewey CN, Henschel R, LeDuc RD, Friedman N & Regev A (2013) De novo transcript sequence reconstruction from RNA-seq using the Trinity platform for reference generation and analysis. Nature Protocols 8: 1494–1512. doi:10.1038/nprot.2013.

Hartfield M, Bataillon T & Glémin S (2017) The evolutionary interplay between adaptation and self-fertilization. Trends in Genetics 33: 420–431. doi:10.1016/j.tig.2017.04.002.

He GP, Qi M, Chen YP, Xu ZY, Luo XB & He BT (2016) Methods for parent apolegamy of Chinese fir in cross breeding. Acta Agriculturae Universitis Jiangxiensis 38: 646–653.

Hedrick PW, Hellsten U & Grattapaglia D (2016) Examining the cause of high inbreeding depression: analysis of whole-genome sequence data in 28 selfed progeny of *Eucalyptus grandis*. New Phytologist 209: 600–611. doi:10.1111/nph.13639.

Hu HZ, Zhang R, Tao ZS, Li XK, Li YY, Huang JF, Li XX, Han X, Feng SQ, Zhang GM & Peng LC (2018) Cellulose synthase mutants distinctively affect cell growth and cell wall integrity for plant biomass production in *Arabidopsis*. Plant and Cell Physiology 59: 1144–1157. doi:10.1093/pcp/pcy050.

Huang HH, Xu LL, Tong ZK, Lin EP, Liu QP, Cheng LJ & Zhu MY (2012) De novo characterization of the Chinese fir (*Cunninghamia lanceolata*) transcriptome and analysis of candidate genes involved in cellulose and lignin biosynthesis. BMC Genomics 13: 648. doi:10.1186/1471-2164-13-648.

Jia SZ, Wang YH, Zhang G, Yan ZM & Cai QS (2021) Strawberry FaWRKY25 transcription factor nega-

tively regulated the resistance of strawberry fruits to *Botrytis cinerea*. Genes 12: 56. doi:10.3390/genes12010056.

Jiang YZ, Tong SF, Chen NN, Liu B, Bai QX, ChenY, Bi H, Zhang ZY, Lou SL, Tang H, Liu JQ, Ma T & Liu HH (2021) The PalWRKY77 transcription factor negatively regulates salt tolerance and abscisic acid signaling in *Populus*. The Plant Journal 105: 1258–1273. doi:10.1111/tpj.15109.

Kanehisa M, Goto S, Kawashima S, Okuno Y & Hattori M (2004) The KEGG resource for deciphering the genome. Nucleic Acids Research 32: 277–280. doi:10.1093/nar/gkh063.

Kimura S & Kondo T (2002) Recent progress in cellulose biosynthesis. Journal of Plant Research 115: 297–302. doi:10.1007/s10265-002-0037-7.

Koonin EV, Fedorova ND, Jackson JD, Jacobs AR, Krylov DM, Makarova KS, Mazumder R, Mekhedov SL, Nikolskaya AN, Rao BS, Rogozin IB, Smirnov S, Sorokin AV, Sverdlov AV, Vasudevan S, Wolf YI, Yin JJ & Natale DA (2004) A comprehensive evolutionary classification of proteins encoded in complete eukaryotic genomes. Genome Biology 5: R7. doi:10.1186/gb-2004-5-2-r7.

Kothari KS, Dansana PK, Giri J & Tyagi AK (2016) Rice stress associated protein 1 (OsSAP1) interacts with aminotransferase (OsAMTR1) and pathogenesis-related 1a protein (OsSCP) and regulates abiotic stress responses. Front Plant Science 7: e1057. doi:10.3389/fpls.2016.01057.

Kristensen TN, Pedersen KS, Vermeulen CJ & Loeschcke V (2010) Research on inbreeding in the 'omic' era. Trends in Ecology & Evolution 25: 44–52. doi:10.1016/j.tree.2009.06.014.

Langfelder P & Horvath S (2008) WGCNA: an R package for weighted correlation network analysis. BMC Bioinformatics 9: 1–13. doi:10.1186/1471-2105-9-559.

Langmead, B & Salzberg SL (2012) Fast gapped-read alignment with Bowtie 2. Nature Methods 9: 357–359. doi:10.1038/nmeth.1923.

Lesaffre T & Billiard S (2020) The joint evolution of lifespan and self-fertilization. Journal of Evolutionary Biology 33: 41–56. doi:10.1111/jeb.13543.

Li AX, Yang WL, Li SG, Liu DC, Guo XL, Sun JZ & Zhang AM (2013) Molecular characterization of three gibberellin-insensitive DWARF1 homologous genes in hexaploid wheat. Journal of Plant Physiology 170: 432–443. doi:10.1016/j.jplph.2012.11.010.

Li B & Colin ND (2011) RSEM: accurate transcript quantification from RNA Seq data with or without a reference genome. BMC Bioinformatics 12: e323. doi:10.1186/1471-2105-12-323.

Liang YC, Reid MS & Jiang CZ (2014) Controlling plant architecture by manipulation of gibberellic acid signalling in *petunia*. Horticulture Research 1: e14061. doi:10.1038/hortres.2014.61.

Liesebach H, Liepe K & Bäucker C (2021) Towards new seed orchard designs in Germany–A review. Silvae Genetica 70: 84–98. doi:10.2478/sg-2021-0007.

Lincoln JE, Sanchez JP, Zumstein K & Gilchrist DG (2018) Plant and animal PR1 family members inhibit programmed cell death and suppress bacterial pathogens in plant tissues. Molecular Plant Pathology 19: 2111–2123. doi:10.1111/mpp.12685.

Liu WX, Zhang FC, Zhang WZ, Song LF, Wu WH & Chen YF (2013) *Arabidopsis* Di19 functions as a transcription factor and modulates PR1 PR2 and PR5 expression in response to drought stress. Molecular Plant 6: 1487–1502. doi:10.1093/mp/sst031.

Liu Y, Xu C, Tang XB, Pei SR, Jin D, Guo MH, Yang M & Zhang YW (2018) Genomic methylation and transcriptomic profiling provides insights into heading depression in inbred *Brassica rapa L ssp pekinensis*. Gene 665: 119–126. doi:10.1016/j.gene.2018.04.047.

Livne S & Weiss D (2014) Cytosolic activity of the gibberellin receptor GIBBERELLIN INSENSITIVE DWARF1A. Plant and Cell Physiology 55: 1727–1733. doi:10.1093/pcp/pcu104.

Lyu JI, Ramekar R, Kim DG, Kim JM, Lee MK, Hung NN, Kim JB, Ahn JW, Kang SY, Choi IY, Park KC & Kwon SJ (2020) Characterization of gene isoforms related to cellulose and lignin biosynthesis in Kenaf (*Hibiscus cannabinus L*) mutant. Plants 9: e631. doi:10.3390/plants9050631.

Mao JP, He ZD, Hao J;Liu TY, Chen JH & Huang SW (2019) Identification, expression, and phylogenetic analyses of terpenoid biosynthesis-related genes in secondary xylem of loblolly pine (*Pinus taeda L*) based on transcriptome analyses. PeerJ 7: e6124. doi:10.7717/peerj.6124.

Matheson AC, White TL & Powell GR (1995) Effects of inbreeding on growth, stem form, and rust resistance in *Pinus elliottii*. Silvae Genetica 44: 37–46.

Martin C & Paz-Ares J (1997) MYB transcription factors in plants. Trends in Genetics 13: 67–73. doi:10.1016/s0168-9525(96)10049-4.

McClosky B, LaCombe J & Tanksley SD (2013) Selfing for the design of genomic selection experiments in biparental plant populations. Theoretical and Applied Genetics 126: 2907–2920. doi:10.1007/s00122-013-2182-x.

McMullen MD, Kresovich S, Villeda HS, Bradbury P, Li H, Sun Q, Flint-Garcia S, Thornsberry J, Acharya C, Bottoms C, Brown P, Browne C, Eller M, Guill K, Harjes C, Kroon D, Lepak N, Mitchell SE, Peterson B, Pressoir G, Romero S, Rosas MO, Salvo S, Yates H, Hanson M, Jones E, Smith S, Glaubitz JC, Goodman M, Ware D, Holland JB & Buckler

ES (2009) Genetic properties of the maize nested association mapping population. Science 325: 737–740. doi:10.1126/science.1174320.

Menzel M, Sletvold N, Ågren J & Hansson B (2015) Inbreeding affects gene expression differently in two self-incompatible *Arabidopsis lyrata* populations with similar levels of inbreeding depression. Molecular Biology and Evolution 32: 2036–2047. doi:10.1093/molbev/msv086.

OuYang F, Mao JF, Wang J, Zhang S & Li Y (2015) Transcriptome analysis reveals that red and blue light regulate growth and phytohormone metabolism in Norway Spruce [*Picea abies (L) Karst*]. PLoS One 10: e0127896. doi:10.1371/journal.pone.0127896.

Paige KN (2010) The functional genomics of inbreeding depression: a new approach to an old problem. BioScience 60: 267–277. doi:10.1525/bio.2010.60.4.5.

Peterson BA, Holt SH, Laimbeer FP, Doulis AG, Coombs J, Douches DS, Hardigan MA, Buell CR & Veilleux RE (2016) Self-fertility in a cultivated diploid potato population examined with the infinium 8303 potato single-nucleotide polymorphism array. The Plant Genome 9: 1-13. doi:10.3835/plantgenome2016.01.0003.

Razanajatovo M, Maurel N, Dawson W, Essl F, Kreft H, Pergl J, Pyšek P, Weigelt P, Winter M & van Kleunen M (2016) Plants capable of selfing are more likely to become naturalized. Nature Communications 7: 1–9. doi:10.1038/ncomms13313.

Ridout MS, Bell JA & Simpson DW (2001) Analysis of segregation data from selfed progeny of allopolyploids. Heredity 87: 537–543. doi:10.1046/j.1365-2540.2001.00938.x.

Robatzek S & Somssich IE (2002) Targets of AtWRKY6 regulation during plant senescence and pathogen defense. Genes & Development 16: 1139–1149. doi:10.1101/gad.222702.

Rymer PD, Sandiford M, Harris SA, Billingham MR & Boshier DH (2015) Remnant *Pachira quinata* pasture trees have greater opportunities to self and suffer reduced reproductive success due to inbreeding depression. Heredity 115: 115–124. doi:10.1038/hdy.2013.73.

Schuetz M, Benske A, Smith RA, Watanabe Y, Tobimatsu Y, Ralph J, Demura T, Ellis B & Samuels AL (2014) Laccases direct lignification in the discrete secondary cell wall domains of protoxylem. Plant Physiology 166: 798–807. doi:10.1104/pp.114.245597.

Shannon P, Markiel A, Ozier O, Baliga1 NS, Wang JT, Ramage D;Amin N, Benno Schwikowski B & Ideker T (2003) Cytoscape: a software environment for integrated models of biomolecular interaction networks. Genome Research 13: 2498–2504. doi:10.1101/gr.1239303.

Sharma S & Shrivastava N (2016) Renaissance in phytomedicines: promising implications of NGS technologies. Planta 244: 19–38. doi:10.1007/s00425-016-2492-8.

Shi JS, Zhen Y & Zheng RH (2010) Proteome profiling of early seed development in *Cunninghamia lanceolata* (Lamb) Hook. Journal of Experimental Botany 61: 2367–2381. doi:10.1093/jxb/erq066.

Shimizu KK & Tsuchimatsu T (2015) Evolution of selfing: recurrent patterns in molecular adaptation. Annual Review of Ecology, Evolution, and Systematics 46: 593–622. doi:10.1146/annurev-ecolsys-112414-054249.

Skibbe M, Qu N, Galis I & Baldwin LT (2008) Induced plant defenses in the natural environment: Nicotiana attenuata WRKY3 and WRKY6 coordinate responses to herbivory. The Plant Cell 20: 1984–2000. doi:10.1105/tpc.108.058594.

Sniezko RA & Zobel BJ (1988) Seedling height and diameter variation of various degrees of inbred and outcross progenies of loblolly pine. Silvae Genetica 37: 50–60.

Tatusov RL, Galperin MY, Natale DA & Koonin EV (2000) The COG database: a tool for genome scale analysis of protein functions and evolution. Nucleic Acids Research 28: 33–36. doi:10.1093/nar/28.1.33.

Ueguchi-Tanaka M, Nakajima M, Motoyuki A & Matsuoka M (2007) Gibberellin receptor and its role in gibberellin signaling in plants. Annual Review of Plant Biology 58: 183–198. doi:10.1146/annurev.arplant.58.032806.103830.

Venegas-Molina J, Proietti S, Pollier J, Orozco-Freire W, Ramirez-Villacis D & Leon-Reyes A (2020) Induced tolerance to abiotic and biotic stresses of broccoli and *Arabidopsis* after treatment with elicitor molecules. Scientific Reports 10: e10319. doi:10.1038/s41598-020-67074-7.

Verma V, Ravindran P & Kumar PP (2016) Plant hormone-mediated regulation of stress responses. BMC Plant Biology 16: e86. doi:10.1186/s12870-016-0771-y.

Vogler DW & Kalisz S (2001) Sex among the flowers: the distribution of plant mating systems. Evolution 55: 202–204. doi:10.1111/j.0014-3820.2001.tb01285.x.

Wang HL, Zhang Y, Wang T, Yang Q, Yang YL, Li Z, Li BS, Wen X, Li WY, Yin WL, Xia XL, Guo HW & Li ZH (2021) An alternative splicing variant of PtRD26 delays leaf senescence by regulating multiple NAC transcription factors in Populus. The Plant Cell 33: 1594–1614. doi:10.1093/plcell/koab046.

Wang TL & Russell JH (2006) Evaluation of selfing effects on western redcedar growth and yield in operational plantations using the tree and stand

simulator (TASS). Forest Science 52: 281–289. doi:10.1093/forestscience/52.3.281.

Wang Z, Gerstein M & Snyder M (2009) RNA-Seq: a revolutionary tool for transcriptomics. Nature Reviews Genetics 10: 57–63. doi:10.1038/nrg2484.

Wang ZM & Chen YT (1988) An analysis on the combining ability of main growth character in Chinese fir and the application of its heterosis. Forest Research 1: 614–624.

Wei T, Simko V, Levy M, Xie Y, Jin Y & Zemla J (2017) Package 'corrplot'. Statistician 56: 316–324.

Weng JK & Chapple C (2010) The origin and evolution of lignin biosynthesis. New Phytologist 187: 273–285. doi:10.1111/j.1469-8137.2010.03327.x.

Willoughby AC & Nimchuk ZL (2021) WOX going on: CLE peptides in plant development. Current Opinion in Plant Biology 63: e102056. doi:10.1016/j.pbi.2021.102056.

Wright SI, Kalisz S & Slotte T (2013) Evolutionary consequences of self-fertilization in plants. Proceedings of the Royal Society B-Biological Sciences 280: e20130133. doi:10.1098/rspb.2013.0133.

Wu HX, Matheson AC & Spencer D (1998) Inbreeding in *Pinus radiata* .I. The effect of inbreeding on growth survival and variance. Theoretical and Applied Genetics 97: 1256–1268. doi:10.1007/s001220051018.

Xie ZL, Nolan TM, Jiang H & Yin YH (2019) AP2/ERF Transcription factor regulatory networks in hormone and abiotic stress responses in *Arabidopsis*. Frontiers in Plant Science 2019 10: e228. doi:10.3389/fpls.2019.00228.

Xu QQ, Wu CT & Xu ZG (2015) Analysis of Chinese fir full diallel progeny genetic variation. Hunan Forest Science Technology 42 :7–12.

Yao S, Wu F, Hao QQ & Ji KS (2020) Transcriptome-wide identification of WRKY transcription factors and their rxpression profiles under different types of biological and abiotic stress in *Pinus massoniana* Lamb. Genes 11: e1386. doi:10.3390/genes11111386.

Yu GC, Wang LG, Han YY & He QY (2012) ClusterProfiler: an R package for comparing biological themes among gene clusters. Omics: A Journal of Integrative Biology 16: 284–287. doi:10.1089/omi.2011.0118.

Yu HH, Du Q, Campbell M, Yu B, Walia H & Zhang C (2021) Genome-wide discovery of natural variation in pre-mRNA splicing and prioritising causal alternative splicing to salt stress response in rice. New Phytologist 230: 1273–1287. doi:10.1111/nph.17189.

Yu RZ (2008) Study on establishing *Cunninghamia lanceolate* breeding populaltion of the third generation. Journal of Forest and Environment 28: 69–72.

Yue LX, Li GL, Dai Y, Sun X, Li F, Zhang SF, Zhang H, Sun RF & Zhang SJ (2021) Gene co-expression network analysis of the heat-responsive core transcriptome identifies hub genes in Brassica rapa. Planta 253: e111. doi:10.1007/s00425-021-03630-3.

Zhang CC, Wang LY, Wei K, Wu LY, Li HL, Zhang F, Cheng H & Ni DJ (2016) Transcriptome analysis reveals self-incompatibility in the tea plant (*Camellia sinensis*) might be under gametophytic control. BMC Genomics 17: e359. doi:10.1186/s12864-016-2703-5.

Zhang CZ, Wang PW, Tang D, Yang ZM, Lu F, Qi JJ, Tawari NR, Shang Y, Li CH & Huang SW (2019) The genetic basis of inbreeding depression in potato. Nature Genetics 51: 374–378. doi:10.1038/s41588-018-0319-1.

Zhang L, Sun HY, Xu T, Shi TY, Li ZY & Hou WQ (2021) Comparative transcriptome analysis reveals key genes and pathways involved in prickle development in eggplant. Genes 12: e341. doi:10.3390/genes12030341.

Zhang M, Liu YH, Xu W, Smith CW, Murray SC & Zhang HB (2020) Analysis of the genes controlling three quantitative traits in three diverse plant species reveals the molecular basis of quantitative traits. Scientific Reports 10: e10074. doi:10.1038/s41598-020-66271-8.

Zhao Q, Nakashima J, Chen F, Yin YB, Fu CX, Yun JF, Shao H, Wang XQ, Wang ZY & Dixon RA (2013) Laccase is necessary and nonredundant with peroxidase for lignin polymerization during vascular development in *Arabidopsis*. The Plant Cell 25: 3976–3987. doi:10.1105/tpc.113.117770.

Zhao Q (2016) Lignification: Flexibility biosynthesis and regulation. Trends in Plant Science 21: 713–721. doi:10.1016/j.tplants.2016.04.006.

Zheng HQ, Hu DH, Wei RP, Yan S & Wang RH (2019) Chinese fir breeding in the high-throughput sequencing era: Insights from SNPs. Forests 10: e681. doi:10.3390/f10080681.

Zheng ZY, Mosher SL, Fan BF, Klessig DF & Chen ZX (2007) Functional analysis of *Arabidopsis* WRKY25 transcription factor in plant defense against pseudomonas syringae. BMC Plant Biology 7: e2. doi:10.1186/1471-2229-7-2.

Zou XY, Liu AY, Zhang Z, Ge Q, Fan SM, Gong WK, Li JW, Gong JW, Shi YZ, Tian BM, Wang YL, Liu RX, Lei K, Zhang Q, Jiang X, Feng YL, Zhang SY, Jia TT, Zhang L, Yuan YL & Shang HH (2019) Co-Expression Network Analysis and Hub Gene Selection for High-Quality Fiber in Upland Cotton (*Gossypium hirsutum*) Using RNA Sequencing Analysis. Genes 10: e119. doi:10.3390/genes10020119.